LOW-TEMPERATURE DEMAGNETIZATION OF NATURAL REMANENT MAGNETIZATION IN DOLERITES OF A PROTEROZOIC DYKE SWARM NEAR NAIN, LABRADOR

ROBERT IAN MACKAY

NOTICE

The quality of this microform is heavily dependent upon the quality of the original thesis submitted for microfilming. Every effort has been made to ensure the highest quality of reproduction possible.

If pages are missing, contact the university which granted the degree.

Some pages may have indistinct print especially if the original pages were typed with a poor typewriter ribbon or if the university sent us an inferior photocopy.

Reproduction in full or in part of this microform is governed by the Canadian Copyright Act, R.S.C. 1970, c. C-30, and subsequent amendments.

AVIS

La qualité de cette microforme dépend grandement de la qualité de la thèse soumise au microfilmage. Nous avons tout fait pour assurer une qualité supérieure de reproduction.

S'il manque des pages, veuillez communiquer avec l'université qui a conféré le grade.

La qualité d'impression de certaines pages peut laisser à désirer, surtout si les pages originales ont été dactylographiées à l'aide d'un ruban usé ou si l'université nous a fait parvenir une photocopie de qualité inférieure.

La reproduction, même partielle, de cette microforme est soumise à la Loi canadienne sur le droit d'auteur, SRC 1970, c. C-30, et ses amendements subséquents.

Canada

Low-temperature demagnetization of natural remanent magnetization in dolerites of a Proterozoic dyke swarm near Nain, Labrador

By

Robert Ian Mackay, B.Sc.

A thesis submitted to the School of Graduate Studies in partial fulfilment of the requirements of the degree of

Master of Science

Department of Earth Sciences (Geophysics)

Memorial University of Newfoundland

Submitted in December, 1994

St. John's Newfoundland

ISBN 0-612-01886-5

Canada

Abstract

Dolerite dykes are presently considered to be the most important recorders of Precambrian paleomagnetism. This is because they can often be accurately dated (using U-Pb in baddeleyite) and can often be shown to carry primary remanence (using the baked contact test). However the mechanisms by which this stable natural remanence is retained over geological time is not well understood. In this thesis, observation of changes in remanence on cooling to 100 K in zero magnetic field and warming back to room temperature is used to help understand these mechanisms.

Twelve specimens were studied from different dykes in a Proterozoic dolerite dyke swarm (U-Pb date of 1,277±3 Ma) located near Nain, Labrador. Each specimen carried a stable westerly-directed remanence that was likely acquired soon after crystallization. Alternating-field demagnetization curves of the natural remanent magnetization (NRM) of each specimen had a quadratic shape. The median destructive field (MDF), which is the alternating field required to reduce intensity by half, ranged from 18mT to 47.5mT for NRM. These properties suggest that remanence is carried by single-domain (SD) or pseudo-single-domain (PSD) grains of magnetite rather than by large multidomain (MD) grains. Median destructive fields were similar for anhysteretic remanent magnetization (ARM) and NRM but were smaller for saturation isothermal remanent magnetization (SIRM).

Apparatus was built to measure remanence intensity as a function of temperature in cooling cycles to near liquid nitrogen temperature. Low-temperature demagnetization experiments were done for NRM, ARM and SIRM for all specimens.

For the three specimens with highest median destructive fields ($\sim$ 40mT for NRM) low temperature cycling had relatively little effect on remanence as expected if the remanence was controlled by shape anisotropy. Similar low-temperature behaviour was reported by others for synthetic magnetites of less than .31μm grain size.

The rest of the specimens showed a pronounced decrease in intensity of remanence on cooling in zero field. The rate of remanence decrease was greatest on approaching 120 K, the temperature of magnetite's Verwey transition from cubic to monoclinic crystal structure. Cooling below the Verwey transition resulted in little further decrease in remanence. On warming back to room temperature remanence increased once the Verwey transition was passed. The final remanence intensity after a cycle of cooling and warming as a function of the initial intensity is termed "recovery" and averaged about $\sim$ 0.75 of initial remanence for NRM and ARM and $\sim$ 0.60 for SIRM. The decrease of ARM on cooling from room temperature to near 120 K is shown to roughly parallel the decrease of saturation magnetostriction, suggesting that remanence decrease is due to unpinning of magnetoelastically controlled domain walls.

Finally, combining our measurements of recovery in magnetite after low-temperature cycling with measurements of others revealed that the higher the median destructive field of the specimen, the higher the recovery. This may be due to both median destructive field and recovery increasing with dislocation density.

Acknowledgements

First I would like to thank my supervisor Dr. Joseph P. Hodych for taking me as a graduate student and supporting me with a stipend from his grant from the Natural Science and Engineering Research Council of Canada (NSERC). I would also like to thank Dr. Hodych for suggesting this thesis topic, supervising the work, and finally for his patience and kindness during my tenure as a Masters candidate.

I am grateful to my parents Dr. Alward and Mrs. Yvonne Mackay for the financial and emotional support during the time I was away from Charlottetown, Prince Edward Island, to pursue this M.Sc. degree.

I also would like to thank Ray Pätzold and Satria Bijaksana for sharing their computer and laboratory expertise which greatly added to my experience and competence and will be useful in future endeavours.

I would like to thank the School of Graduate Studies of Memorial University of Newfoundland for a Graduate Fellowship during the 1993 academic year.

I would also like to thank Dr. J.P. Hodych, Dr. G.S. Murthy, Dr. H.G. Miller, Dr. M.G. Rochester and Dr. J. Hall for their instruction in my graduate courses.

I would like to thank my office mates Behnam Seyed-Mahmoud, Ron Wiseman and Ian Leslie for academic help and friendship during my 28 month period in St. John's, Newfoundland.

Finally I would like to thank my Aunt Barbara Hardy for her friendship and also for helping find the apartment that I lived in during my M.Sc. candidacy.

Table of Contents

Page

Page

List of Tables

List of Figures

Page

Page

List of Abbreviations and Nomenclature

NRM : Natural Remanent Magnetization

ARM : Anhysteretic Remanent Magnetization

SIRM: Saturation Isothermal Remanent Magnetization

MD : Multidomain

SD : Single-domain

PSD : Pseudo-single-domain

MDF : Median destructive field

AF : Alternating-field

H_c : Coercive force

M_s : Saturation magnetization

T_v : Verwey crystallographic transformation temperature ($T_v \approx$ 110-120 K).

T_k : temperature at which $K_1=0$ "Isotropic point" ($T_k \approx$ 130 K).

λ_{111}: Saturation magnetostriction along [111] crystal axis.

λ_{100}: Saturation magnetostriction along [100] crystal axis.

λ_s : Akulov approximation for polycrystalline saturation magnetostriction.

K_1 : The magnetocrystalline anisotropy coefficent of degree 2.

K_2 : The magnetocrystalline anisotropy coefficent of degree 3.

K_{eff}: $.115K_1+.021K_2$

A : Exchange constant.

dw : Domain wall width.

Chapter One

Introduction

1.1 Current concepts in remanence retention in magnetite

The stability of thermal remanent magnetization (TRM) of terrestrial igneous rocks is thought by many paleomagnetists to reside primarily in magnetite, or titanomagnetite grains that are small enough to sustain equilibrium single domain (SD) structures [*Evans and McElhinny*, 1969; *Heider et al.*, 1988]. The qualitative argument is that coercivity of magnetic moments associated with SD particles is governed by shape anisotropy, which usually outweighs the coercivities of domain walls in grains large enough to equilibrate as multi-domain (MD) structures [*Day*, 1977; *Dunlop*, 1986; *Heider*, 1990]. However, *Stacey* [1963] pointed out that most igneous rocks that have stable TRM have a larger proportion of MD grains than previously believed. To explain stable TRM in paleomagnetic specimens containing mostly MD grains, *Stacey* [1963] coined the term "pseudo-single-domain" (PSD) for grains which have the stability expected of SD grains but equilibrate with domain walls present.

It must be pointed out that whereas theories governing the stability of TRM in SD particles are well developed [*Moon and Merrill*, 1988], theories for PSD particles are still relatively poorly developed [*Dunlop*, 1986; *Dunlop and Argyle*, 1991; *Xu and Merrill*, 1992]. Theories for stable TRM in MD grains are also poorly developed [*Xu and Merrill*, 1989, 1990, 1992; *Moskowitz*, 1993]. The evolving concept is the one put forth originally by *Verhoogen* [1959] that the coercivity of TRM may be controlled by internal stresses, and that these internal stresses are perhaps stress gradients associated with

dislocations causing magnetoelastic interaction with domain walls [*Syono*, 1965; *Shive*, 1969; *Xu and Merrill*, 1989, 1990, 1992; *Moskowitz*, 1993].

An effective method for separating the various anisotropies governing the stability of remanence in magnetite-bearing specimens is to study change in magnetic parameters on cooling down to liquid nitrogen temperature (77 K) [*Hodych*, 1982, 1986, 1990; *Xu and Merrill*, 1992]. On cooling, the specimens first pass through the isotropic point ($T_K \approx 130$ K), where the magnetocrystalline anisotropy constant K_1 for magnetite passes through zero on changing sign [*Syono*, 1965]. Then, they pass through the Verwey transition ($T_V \approx 120$ K), where magnetite's crystal structure changes from cubic to orthorhombic [*Syono*, 1965]. Low-temperature cycling of remanence can also provide a simple, non-destructive method to identify magnetite as a remanence carrier as has been done for limestones by *Mauritush and Turner* [1975]. It has also been used to discriminate between magnetosomes produced anaerobically by magnetotactic bacteria and magnetosomes produced by dissimilatory iron reducing bacteria [*Moskowitz et al.*, 1989], by observing either a change in remanence intensity over T_K or T_V respectively.

Ozima et al. [1964] pointed out that the demagnetization by low-temperature cycling might be an effective and safer alternative to thermal demagnetization (with its risk of chemical alteration), and alternating field demagnetization (with its risk of anhysteretic remanence acquisition). Low-temperature demagnetization looked promising since most unstable TRM components residing in MD grains of magnetite were thought to be controlled by K_1 [*Strangway et al.*, 1968]. However, *Merrill* [1970] pointed out that

some unstable TRM might have coercivities controlled by stress and thus be less affected by low-temperature cycling through T_K. Hence, NRM surviving after low-temperature demagnetization might still have unstable components, whereas alternating field demagnetization destroys all remanence with coercivities less than the peak alternating field, regardless of what mechanisms control the coercivity. As a result, low-temperature demagnetization is not an effective cleaning method [*Heider et al.*, 1992]. However, a significant contribution to our understanding of the mechanisms controlling magnetic stability has come from studying coercivity and remanence intensity on cooling down to liquid nitrogen temperatures.

Hodych [1982, 1986], with natural specimens, and *Dunlop and Argyle* [1990], with synthetic specimens, showed that coercive force of magnetite can vary in approximate proportion to λ_s/M_s on cooling, (where λ_s is the Akulov approximation saturation magnetostriction and M_s is saturation magnetization). *Xu and Merrill* [1992] showed in a review of available experimental data that this proportionality exists for many specimens between the Verwey temperature and the Curie temperature. They also agreed with the findings of *Argyle and Dunlop* [1990] that for SD grains this proportionality does not exist, (except in the case of non-stoichiometric SD grains with high Ti^{+4} content [*Worm and Markert*, 1987], which show proportionality to λ_{100} on cooling). *Hodych* [1982, 1986] and *Argyle and Dunlop* [1990] showed that K_1 control of H_c on cooling does not seem common.

Hodych [1982, 1986] suggested that the decrease in H_c on cooling was due to a

decrease in λ_s lowering barriers to domain walls pinned by internal stresses. *Xu and Merrill* [1992] went further by suggesting that the stress fields of dislocations cause the magnetoelastic interaction with domain walls. The relationship between crystal defects and hysteresis parameters is well documented [*Kittel*, 1949], and annealing experiments on synthetic magnetite [*Dankers and Sugiura*, 1981; *Smith and Merrill*, 1984] have shown that hysteresis parameters (such as H_c) are reduced after heat treatment. *Shive and Butler* [1969] argued theoretically that if exsolution has occurred, the magnetoelastic energy associated with the misfit at the magnetite-ilmenite lamellae boundaries cannot account for the high coercivity of magnetite. However *Shive* [1969] indicated that dislocation densities are high near the misfit; hence the concepts put forth by *Xu and Merrill* [1992] and *Moskowitz* [1993] suggest that domain walls can be effectively pinned at such boundaries.

Low-temperature demagnetization experiments will be reviewed in the next chapter. As we shall see, SD magnetite is usually expected to show little change in remanence intensity on cooling to liquid nitrogen temperatures. MD magnetite usually demagnetizes very significantly in low-temperature cycles. PSD magnetite has an intermediate response to low-temperature cycling. Low-temperature demagnetization experiments can thus help identify the mechanism by which stable remanence is held in magnetite and this is what we will exploit in this thesis.

1.2 Typical multidomain and single-domain behaviour in mafic igneous rocks

Many Precambrian dolerite dyke swarms of the Canadian Precambrian Shield

have been shown to carry primary remanence (using baked contact tests). Many of these dyke swarms also yield accurate U-Pb ages making them very useful in defining polar wander paths for the Precambrian Canadian Shield [*Buchan and Halls*, 1990]. However, there is some dispute as to whether primary remanence in such mafic igneous rocks is held primarily in SD or in MD grains. Many authors [*Lowrie and Fuller*, 1971; *Dunlop et al.*, 1973; *Evans and McElhinny*, 1969; *Heider et al.*, 1988; *Strangway et al.*, 1968] contend that stable remanence is primarily due to SD grains of magnetite or titanomagnetite dominated by shape anisotropy. Others [*Hodych*, 1982] contend that MD grains with magnetostrictive control of remanence are also important.

Lowrie and Fuller [1971] proposed a simple test for paleomagnetists to discriminate between remanence held in SD and MD grains. The test involved comparing weak-field TRM and strong-field TRM or SIRM. The median destructive field (alternating field required to reduce remanence intensity by half) of the weak-field TRM in rocks whose remanence was held in SD or PSD grains was harder than its strong-field TRM, whereas the reverse was be true for MD grains $> 10\text{-}15\mu m$. They also concluded from the natural specimens used in their study that stable remanence held in large MD grains was rare, a finding agreed upon by most texts in paleomagnetism [*e.g. Tarling*, 1984]. However true SD grains are also likely rare due to their narrow size range [*Dunlop*, 1990]. Thus stable remanence must dominantly reside in PSD grains or in small MD grains. This is supported for example by the experiments of *Hodych* [1991] in which SIRM of magnetite-bearing rocks decreased in rough proportion to λ_s on cooling to T_v,

suggesting that remanence was controlled by internal stresses impeding domain wall movement.

1.3 Significance to Proterozoic paleomagnetism of the Canadian Precambrian Shield.

Proterozoic mafic dyke swarms yield the majority of the firmly determined paleomagnetic poles for the Canadian Precambrian Shield [*Buchan and Halls*, 1990]. Of the 60 Proterozoic dyke swarms that have been geologically identified, 40 had been studied paleomagnetically by 1990 and 20 of these had tests to verify that a primary remanence exists (baked contact tests). With the advent of U-Pb zircon and baddeleyite radiometric dating, a precise age can often be attached to paleopoles from mafic dyke swarms helping greatly to define apparent polar wander paths. By 1990, the 20 major dyke swarms that had tests verifying primary remanence, 8 had precise dating using the U-Pb zircon or baddeleyite method [*Buchan and Halls*, 1990].

A paleomagnetic study has not yet been completed for the Nain dolerite dyke swarm. However, oriented samples were collected by K.L Buchan and J.P. Hodych from 39 sites. One or two specimens have been studied paleomagnetically from each site and many of these were stably magnetized and of high coercivity. Baked contact tests are in progress. There is also a U-Pb age of 1277±3 Ma for the east-west trending dykes (*J.C. Roddick*, private communication, 1994). All the specimens studied in this thesis were from the east-west dykes. The paleopole from this study should help delineate the ascending track of the Logan Loop in the Proterozoic apparent polar wander path for the Canadian Shield.

Chapter Two

Review of Literature on Low-temperature Demagnetization

2.1 Behaviour of magnetite remanence in cooling cycles to 77 K

While cooling to liquid nitrogen temperature (77 K), stoichiometric magnetite passes through the "isotropic point" (T_k) at 130 K where the magnetocrystalline anisotropy constant K_1 changes sign from positive to negative [*Kakol et al.*, 1991]. At 120 K, the Verwey transition temperature (T_v), magnetite transforms from cubic to monoclinic crystal structure [*Verwey*, 1939; *Zuo et al.*,1990]. It has been reported that remanence intensity held in magnetite grains can change markedly at T_k [*Kobayashi and Fuller*, 1968; *Merrill*, 1970; *Boyd et al.*, 1984; *Jarrard and Halgedahl*, 1990; *Heider et al.*, 1992; *Borradaile*, 1994] or at T_v [*Creer*, 1967; *Aragon et al.*, 1985; *Moskowitz et al.*, 1989; *Hodych*, 1991; *Özdemir et al.*, 1993]. Whether this marked change in remanence intensity is observed over T_k or T_v depends not only on the grain size but the type of remanence [*Argyle and Dunlop*, 1990; *Levi and Merrill*, 1976, 1978] and on the crystalline imperfections in the magnetite grains that hold the remanence [*Parry* 1979, 1980; *Heider et al.*, 1992; *Borradaile*, 1994]. Note that it may be difficult to determine whether the change is observed over T_k or T_v because of the small difference in temperature between them (10°) and because both temperatures can be lowered by small additions of Ti [*Syono*, 1965] or by oxidation [*Özdemir et al.*, 1993].

a.) Single-domain magnetite

For SD magnetite grains (diameter $\approx$ 0.05-0.08μm [*Moon and Merrill*, 1984;

Butler, 1992]), remanence is usually controlled by shape anisotropy and is directed along the long axis of the grain. The specimen's remanence intensity on cooling to T_v can only change due to the thermal change of M_s [*Worm and Markert*, 1986], but M_s only changes by about 6% between 300 K and 130 K [*Pauthenet*, 1950]. Only for nearly spherical grains would magnetocrystalline anisotropy be expected to outweigh shape anisotropy and lead to a change in remanence intensity at T_k as observed by *Schmidbauer and Schembera* [1987]. Even a 10% deviation from spherical grain shape should allow shape anisotropy to outweigh magnetocrystalline anisotropy and almost totally suppress remanence change at T_k [*Argyle and Dunlop*, 1990]. However SD magnetite grains whose coercivity is controlled by shape anisotropy may show a marked change in remanence intensity over T_v, provided the Verwey transition is not suppressed by Ti content or oxidation of the magnetite [*Özdemir et al.*, 1993].

Remanence held in SD magnetite regains its initial intensity after low-temperature cycling; that is "recovery" (final divided by initial remanence intensity) is nearly 100% [*Dunlop and Argyle*, 1991; *Heider et al.*, 1992]. It has been shown that any dramatic change in remanence held in typical SD grains on cooling to low temperatures is at the crystallographic transition T_v at 110-120 K [*Özdemir et al.*, 1993]. On cooling, remanence should be controlled first by shape anisotropy and then, below the crystallographic transition at T_v, remanence may be dominated by the magnetocrystalline anisotropy associated with the monoclinic structure. On warming back through T_v, the crystal structure would then revert back to cubic and remanence should again be

controlled by shape anisotropy. Since cooling and warming through T_k or T_v has no real effect on shape anisotropy, recovery should virtually be complete, which was shown to be the case for SIRM held in the magnetite grains with mean diameters of 0.037μm-0.10μm studied by *Heider et al.* [1992], and for the SD grains of *Levi and Merrill* [1976]. Note that for grain sizes less than .037μm, the Verwey transition can be suppressed by the effects of superparamagnetism [*Özdemir et al.*,1993], explaining the findings of *Moskowitz et al.* [1989] whose 0.010μm magnetite grains of dissimilatory iron-reducing bacteria showed no change in remanence intensity at T_v.

b.) Multidomain magnetite

For multidomain (MD) magnetite grains greater than 10μm in diameter, remanence intensity may change on passing through either T_k or T_v. The physical mechanisms of how remanence is demagnetized on cooling and recovered on warming through these transition points can be varied. *Heider et al.* [1992] and *Dunlop and Argyle* [1991] proposed that the mechanism of low-temperature demagnetization in MD magnetite is the unpinning of domain walls near T_k, since domain wall width dw α $[A/K_{eff}]^{1/2}$ [*Landau and Lifshitz*, 1935], where $K_{eff}=.115K_1+.021K_2$ and A is the exchange constant. Thus, when $K_1=0$, domain walls become large and are no longer effectively pinned in stress regions associated with dislocations, since according to theory [*Xu and Merrill*, 1989] domain walls need to be 1/5 the wavelength of stress in order to be pinned. However *Boyd et al.* [1984] observed, for a magnetite grain of about 20μm holding SIRM, that before low-temperature cycling through T_k no domain wall existed.

After cycling to liquid nitrogen temperature, he observed that a domain wall had nucleated, which he interpreted as being caused when $K_1=0$ and magnetostatic effects outweighed net K_{eff} (*Brown condition*). That is, he assumed that remanence intensity of the grain dropped at or near T_k. On the other hand, *Nagata* [1967], *Creer* [1967], *Hodych* [1991] and *Özdemir et al.* [1993] observed a change in remanence intensity at T_v as opposed to T_k. *Hodych* [1991] suggested that the gradual demagnetization in MD magnetite from room temperature to near T_v is caused by a decrease in coercive force which is magnetostrictively controlled through internal stresses. In support, he pointed out that remanence decreased in approximate proportion to coercive force and magnetostriction on cooling to near T_v. At T_v, a marked drop in remanence intensity was observed, which Hodych assumed to be due to the crystallographic transition causing a restructuring of domains. A marked intensity drop on cooling through T_k did not seem to be observed. This could be due to stress-induced magnetoelastic anisotropy associated with crystalline imperfections impeding domain wall expansion when $K_1=0$ [*Kobayashi and Fuller*, 1968; *Heider et al.*, 1992].

The following model could explain why some specimens show a marked remanence decrease at T_v whereas the decrease might be at T_k in other specimens. Suppose remanence is carried by strongly pinned domain walls (*magnetoelastic anisotropy energy*) and weakly pinned walls (*magnetocrystalline anisotropy energy*). While cooling to T_k, weakly pinned domain walls may broaden enough to move out of stress regions if their width becomes 1/5 the wavelength of stress associated with a

dislocation or other crystalline imperfection [*Xu and Merrill*, 1989]. However, domain walls that are strongly pinned by stress-induced magnetoelastic anisotropy, $\lambda\sigma$, (λ being some combination of single crystal saturation magnetostriction λ_{100} and λ_{111} and σ representing stress [*Heider et al.*, 1992]), may not become wide enough to unblock when $K_1=0$ at T_k. Some of these strongly pinned walls may however unblock when the crystallographic change at T_v forces domain reorganization, remanence being governed by the magnetocrystalline easy direction associated with the monoclinic crystal structure. Thus the observation of a large remanence decrease at T_k or T_v in large MD crystals of magnetite may depend on how perfect the crystal is with high dislocation densities, a large decrease in remanence would be expected on cooling through T_v, whereas with low dislocation densities, a large decrease in remanence could occur on cooling through T_k.

Some support for the above model can be obtained from the observations of *Hodych* [1991] whose magnetite-bearing rock specimens (*mainly mafic rocks*) of high coercivity (between 2-15mT) showed a marked decrease in intensity on cooling through T_v, whereas his one specimen of low coercivity (1.1mT) showed a marked decrease on cooling through T_k. The low coercivity specimen may have had a lower dislocation density since coercivity has been shown to increase in magnetite if the specimens are crushed, ground or quenched from high temperatures [*Lowrie and Fuller*, 1969; *Dankers and Sugiura*, 1981; *Boyd et al.*, 1984]. The Verwey transition was also observed in a 1.5mm natural single crystal [*Özdemir et al.*, 1993] , while a dramatic remanence change at T_k has been reported in synthetically grown magnetite [*Schmidbauer and Schembera*,

1987]. This possible difference between natural and synthetic specimens may be due to the fact that natural magnetite often have high dislocation densities [*Shive*, 1969; *Xu and Merrill*, 1992] whereas hydrothermally grown synthetic magnetite have lower dislocation densities [*Heider et al.*, 1992].

High stress associated with dislocations or other crystalline imperfections in MD magnetite can effect the amount of recovery of remanence after a cooling cycle to liquid nitrogen temperatures [*Levi and Merrill*, 1976, 1978; *Parry*, 1979, 1980; *Heider et al.*, 1992]. *Kobayashi and Fuller* [1968] showed that increasing stress applied to polycrystalline nickel and cobalt increased the amount of remanence recovered. *Heider et al.* [1992] demonstrated that recovery increased with stress by performing low-temperature demagnetization experiments on magnetite with different initial stress states (changing the stress state either by annealing at 600°C or quenching from 600°C to -196°C). *Parry* [1979, 1980] showed that recovery of SIRM and TRM after a low-temperature cycle depends on grain size for magnetite grains (of 1.5-220μm in diameter), the smaller the grain size the larger the recovery. However, *Heider et al.* [1992] thought that the recovery of Parry's larger grain size samples was intrinsically related to internal stresses as opposed to grain size since magnetite greater than 10μm in diameter with low internal stress showed no dependence of recovery on grain size, whereas true dependence of recovery on grain size exists for TRM and SIRM of magnetite less than 1μm in diameter [*Levi and Merrill*, 1976, 1978; *Argyle and Dunlop*, 1991] and extends to the upper limit for PSD effects [*Heider et al.*, 1992]. Compare Tables 2.0 and 2.1.

The physical mechanism of how internal stresses can increase recovery of remanence in MD magnetite was suggested by *Kobayashi and Fuller* [1968] and *Heider et al.* [1992]. On cooling from room temperature, magnetization of a particular domain will be along a magnetocrystalline easy direction (along <111> axis) until T_k when remanence direction will shift to the nearest magnetoelastically controlled easy axis. Then, on further cooling to T_v, remanence direction will shift again to the magnetocrystalline easy direction associated with the monoclinic structure. On warming back through T_v, remanence direction is controlled once again by the magnetoelastically controlled easy axis until T_k when the remanence direction is controlled by the magnetocrystalline anisotropy easy direction of the cubic crystal structure. In other words, the higher the amount of internal stresses caused by dislocations the higher the probability that the original domain structure will be recovered. If the dislocation density is high, much the same is expected except that there should be little remanence change at T_k. Figure 2.0 illustrates the typical low-temperature behaviour of large multidomain magnetite grains. The 230μm grains were made by crushing and sieving a natural magnetite crystal by *Hodych* [1986]. The room temperature coercive force of his sample was low (about 3.2mT). These larger MD grains exhibit a large decrease in SIRM on cooling. The decrease roughly parallels that of λ_{111} (shown by the solid line of Figure 2.0). Recovery of SIRM is low (about 20%) as expected of the low dislocation density suggested by the low coercive force.

B.) Pseudo-single-domain magnetite

Fine magnetite grains that are in theory too large to equilibrate as SD structures but still have SD-like moments are called pseudo-single-domain (PSD) grains (diameter $\approx$ 0.10μm - 15μm [*Dunlop*, 1990]). Remanence held in PSD grains can be shown to have a recovery, after a low-temperature cycle, that is intermediate between that of the high recovery of SD grains and the low recovery of MD grains [*Levi and Merrill*, 1976, 1978]. *Levi and Merrill* found that if the magnetite grains were <0.31μm in diameter, the shape of alternating field demagnetization curves were very similar for ARM and TRM and the recovery of initial remanence after low-temperature cycles was very similar for ARM and TRM (between 93% and 100% recovery). However for magnetite grains >0.31μm in diameter, recovery was greater for TRM (about 59% for both their 1.5μm & 2.7μm specimens) than for ARM (56% and 41% for the 1.5μm and 2.7μm specimens respectively) and alternating field demagnetization was harder for TRM than for ARM. However they did not study grain sizes between 0.31μm and 1.2μm. *Argyle and Dunlop* [1990] studied the recovery of weak-field TRM, ARM and SIRM of grain sizes between .215μm and .540μm and found that recovery of TRM was between 75% - 45% , recovery of ARM was 68% - 35% and recovery of SIRM was 44% - 23%. Recovery of remanence after low-temperature demagnetization of sub-micron PSD grains was interpreted to be size dependent-recovery increasing as grain size decreased. *Heider et al.* [1992] showed that this size dependency extended to the upper limits of PSD effects (10μm). Recovery observed in these and related experiments is summarized in Table 2.1.

Dunlop and Argyle [1991] demonstrated that the stable remanence in PSD grains of magnetite reside within SD-like regions of the grain. They showed that the AF demagnetization curve of remanence that *recovered after low-temperature cycling* of hydrothermally grown magnetite with mean diameters .215μm, .390μm and .540 μm had the *quadratic shape* that is characteristic of SD grains whose coercivity is controlled by shape anisotropy. Thus the recovered remanence was shown to reside in this SD-like fraction whereas the MD-like fraction was demagnetized by low-temperature cycles. The shape of the demagnetization curve of the SD-like fraction was found to be independent of PSD grain size and this remanence showed nearly complete recovery.

The fact that low-temperature cycles caused demagnetization for grain size greater than .31μm [*Levi and Merrill*, 1976] indicates that some mechanism other than magnetostatic energy is pinning the domain walls. *Argyle and Dunlop* [1990] showed for their .540μm hydrothermally grown sample that H_c varied in proportion to λ_s/M_s on cooling, which suggests that domain walls were magnetoelastically pinned despite dislocation densities likely being low. This is not well accounted for by the theory of *Xu and Merrill* [1992] in which magnetoelastic control of domain walls can exist in grains as small as 1μm, if dislocation densities are large. More evidence for magnetoelastic pinning of domain walls in small magnetite grains comes from *Heider et al.* [1992] who showed that heating that presumably decreases dislocation densities also decreases recovery of SIRM in magnetite of 0.57μm to 6.3μm diameter.

The observation of remanence change at T_v and T_k for remanence held in PSD

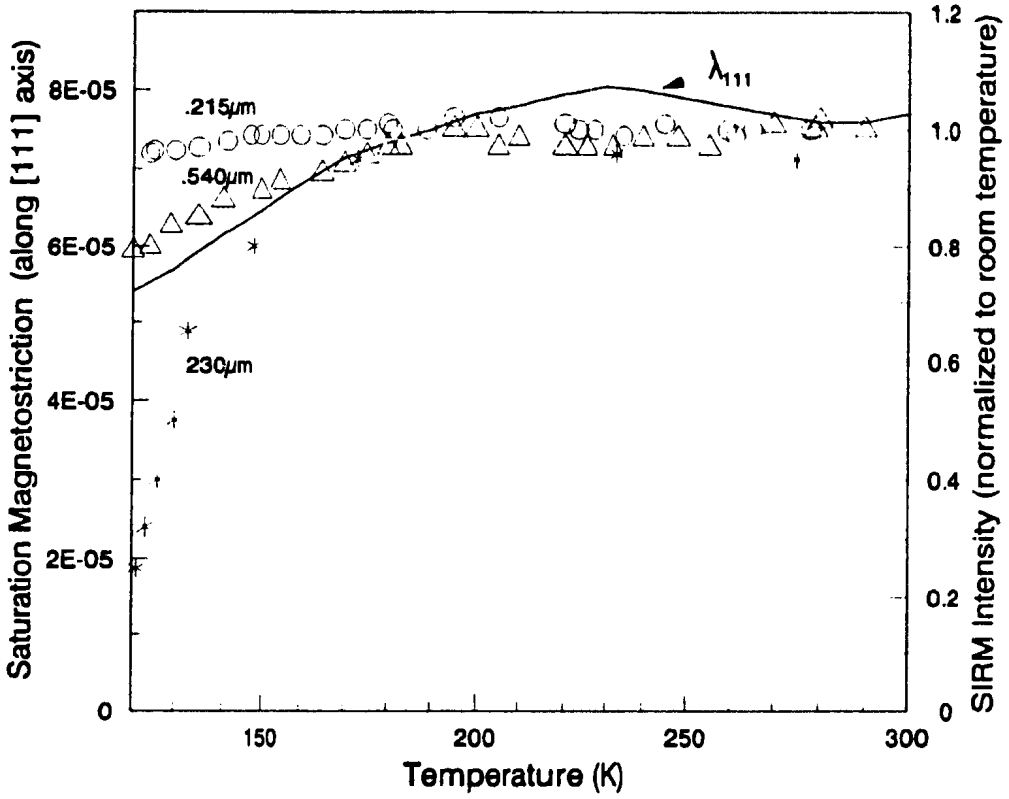

Fig 2.0 Change of SIRM reported by other workers on cooling compared to saturation magnetostriction

grains has not been as well documented as for MD grains. *Boyd et al.* [1984] argued that the effect of the isotropic point is totally suppressed in magnetite grains less than 1μm because domain walls cannot be nucleated, whereas *Schmidbauer and Schembera* [1986]observed remanence change at T_k for magnetite particles in the SD grain range (.061μm-.162μm). For the .540μm synthetic magnetite of *Argyle and Dunlop* [1990], intensity of remanence was measured from 300 K down to 100 K and they observed neither the isotropic point nor the Verwey transition, which suggests that somehow these transitions were displaced to lower temperatures.

Figure 2.0 illustrates the behaviour of SIRM held in fine-grained magnetite of known size. The .215μm and .540μm magnetite were grown by *Argyle and Dunlop* [1991] using a hydrothermal recrystallization technique. The room temperature coercivities were 7.5mT and 5.5mT for the .215μm and .540μm grain sizes respectively. As illustrated, the variation of SIRM in the .215μm grains shows little change on cooling, most likely due to the coercivity of these grains being controlled by shape anisotropy. The .540μm grains however do show a small decrease on cooling similar to that of λ_{111} (shown by the solid line of Figure 2.0) which might be due to partial magnetoelastic control of coercivity.

Poor crystallinity or the presence of externally applied stress have some of the same effects on recovery in low-temperature cycling for PSD grains as they do for MD grains. Basically the higher the internal stress, the higher the recovery of initial remanence [*Heider et al.*, 1992].

Table 2.0 Illustrates how recovery of remanence after low temperature cycles to 77 K shows little size dependence for larger *multidomain* (MD) magnetite grains (> > 10μm), but may depend on whether the grains were stressed (* indicates specimens with large internal or external stress)

Source	<d> (μm)	MDF (TRM)	R_T	MDF (SIRM)	R_S
Heider et al.,(1992)	11	12	.08	6.3	.04
Parry (1979)*	15			10	.38
Heider et al.,(1992)*	20	25	.28	11.7	.21
Heider et al.,(1992)*	25	24	.18	11.9	.16
Parry (1979)*	37			8.4	.30
Heider et al.,(1992)*	64	18	.06	9.7	.13
Heider et al.,(1992)	94	16		10.9	.13
Parry (1979)*	100			5.6	.17
Parry (1979)*	220			5.0	.16
Heider et al.,(1992)	356	4-5		6.8	.15

Definition of columns:

<d> : is mean grain diameter.
MDF : is median destructive field of AF-demagnetization curves given in millitesla.
R_T : Recovery of thermal remanence after cooling cycles to 77 K.
R_S : Recovery of isothermal saturation remanence after cooling cycles to 77 K.

Note: This table shows the effects of internal stresses on recovery after low-temperature cycling through 77 K. The specimens of *Parry* [1979] were ball milled from a larger magnetite crystal which likely set up high internal stresses in the resulting fine magnetite grains. Also all of the specimens of *Heider et al.* [1992] were hydrothermally grown so that his 11μm, 94μm and 356μm specimens should be mostly stress free but his specimens 20μm, 25μm and 64μm were then hydraulically pressed and should have a high dislocation density. The stressed specimens tend to show a recovery that is size dependent if the magnetite grains are much larger than 10μm. The specimens with low stress do not tend to show a dependence of the magnetite grain size.

Table 2.1 Illustrates how recovery of remanence after low temperature cycles to 77 K increases with decreasing grain size for *pseudo-single-domain* (PSD) grains of magnetite. (* represents the specimens that have externally applied stress or internal stresses).

Source	<d> (μm)	MDF (TRM) mT	R_T	MDF (ARM) mT	R_A	MDF (SIRM) mT	R_S
Levi & Merrill,(1978)	.120	28	.986	23	.980		
Levi & Merrill,(1978)	.210	37	.990	36	.978		
Dunlop & Argyle,(1991)	.215	15	.770	18.7	.680	13	.440
Levi & Merrill,(1976)	.240	34	.945	37	.980		
Dunlop & Argyle,(1991)	.390	11.2	.570	15.8	.480	10	.280
Dunlop & Argyle,(1991)	.540	12.2	.480	15.5	.351	11.2	.230
Heider et al.,(1992)*	.570	50	.900			13.3	.890
Heider et al.,(1992)	.760	16	.460			11.3	.260
Levi & Merrill,(1978)	1.50	14.2	.593	15	.561		
Levi & Merrill,(1978)	2.70	8.2	.590	5.8	.413		
Parry, (1979)*	4.50					9.6	.450
Heider et al.,(1992)*	4.60	14	.150			10.6	.420
Heider et al.,(1992)	6.30	14	.100			9	.140

Definition of columns: same as Table 2.0.

R_A : Recovery of anhysteretic remanence after cooling cycles to 77 K.

Note: Compare the .540μm magnetite used by *Dunlop and Argyle* [1991], which was grown by the hydrothermal recrystallization technique, which should result in low internal stress and low recovery (0.23), and the .570μm magnetite of *Heider et al.* [1992], which was hydraulically pressed to induce internal stresses, thus causing a higher recovery (0.89).

Chapter Three

Apparatus for low-temperature demagnetization

Apparatus was constructed to measure how remanence of rock specimens in zero magnetic field varies during cooling to near liquid nitrogen temperature (77 K) and warming back to room temperature. The apparatus consists of a fluxgate magnetometer to measure remanence, a magnetic shield to provide a field-free space and a temperature control assembly to vary the specimen's temperature.

3.0 The magnetometer and magnetic shielding

Remanence was measured with a modified Schonstedt portable magnetometer (*model PSM-1*). This magnetometer's fluxgate probe was moved from its original field-free space (13 cm in length and 8.5 cm diameter) to a much larger field free space (52 cm in length and 20 cm in diameter) provided by a nested set of 5 high permeability metal cylindrical cans open at one end (Figure 3.0).

The specimen is held by a tube of pyrex which itself is connected to a 360° dial which rests on an external platform. Turning the dial rotates the rock specimen with respect to the fluxgate element, causing a deflection of the meter needle in the magnetometer. The fluxgate element is positioned at the same height as the specimen to maximize the signal.

3.1 Temperature control assembly

This part of the apparatus (shown in detail in Figure 3.1) varies the specimen's temperature, allowing it to be cooled from room temperature to 93 K, and then to be

warmed back to room temperature. The temperature control assembly is enclosed in a 1 litre capacity Dewar flask which holds the liquid nitrogen during the experiment, providing specimen cooling and also insulating the fluxgate element which lies outside this Dewar flask. A second smaller Dewar flask is placed inside the 1 litre Dewar. A high resistance wire (Chromel A) is wound non-inductively and glued to the inside wall of this inner Dewar using a non-magnetic castable ceramic (Cermacast 250). The temperature inside the inner Dewar can then be adjusted by varying the AF current through the heating element using a variac (*General Radio Company, type W10MT 3A*). The rock specimen is held in the inner Dewar and its temperature can be varied between room temperature and 93 K. (The vacuum in the inner Dewar had to be adjusted initially to allow 93 K to be reached). G.M. English is thanked for donating the inner Dewar which he originally constructed for temperature control on a hysteresis loop plotter.

The inner Dewar is held fixed inside the 1 litre Dewar by a polystyrene stopper, which also helps insulate the liquid nitrogen bath inside the 1 litre Dewar. A float was used to monitor the liquid nitrogen level in the 1 litre Dewar (Figure 3.0).

The distance the specimen is suspended from the bottom of the inner Dewar is determined by where the temperature gradient along the length of the Dewar is a minimum, which is shown in *Section 3.2b* to be 1 cm from the inside bottom of the inner Dewar. Minimizing temperature gradient should minimize any smearing of important transitions of magnetite on cooling.

Temperature was monitored using two copper-constantin thermocouples (*T-type*

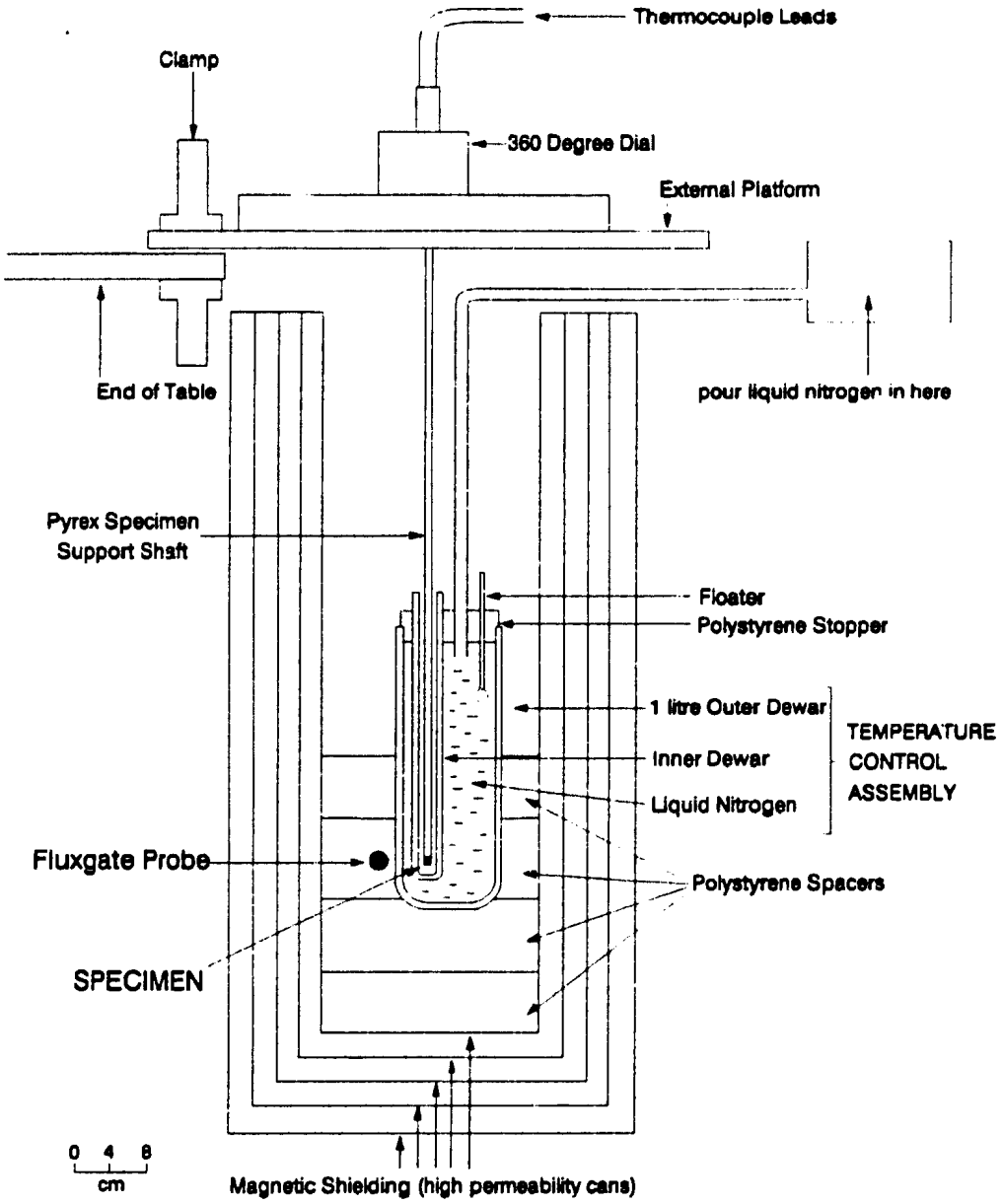

Fig 3.0 Apparatus for Low Temperature Demagnetization

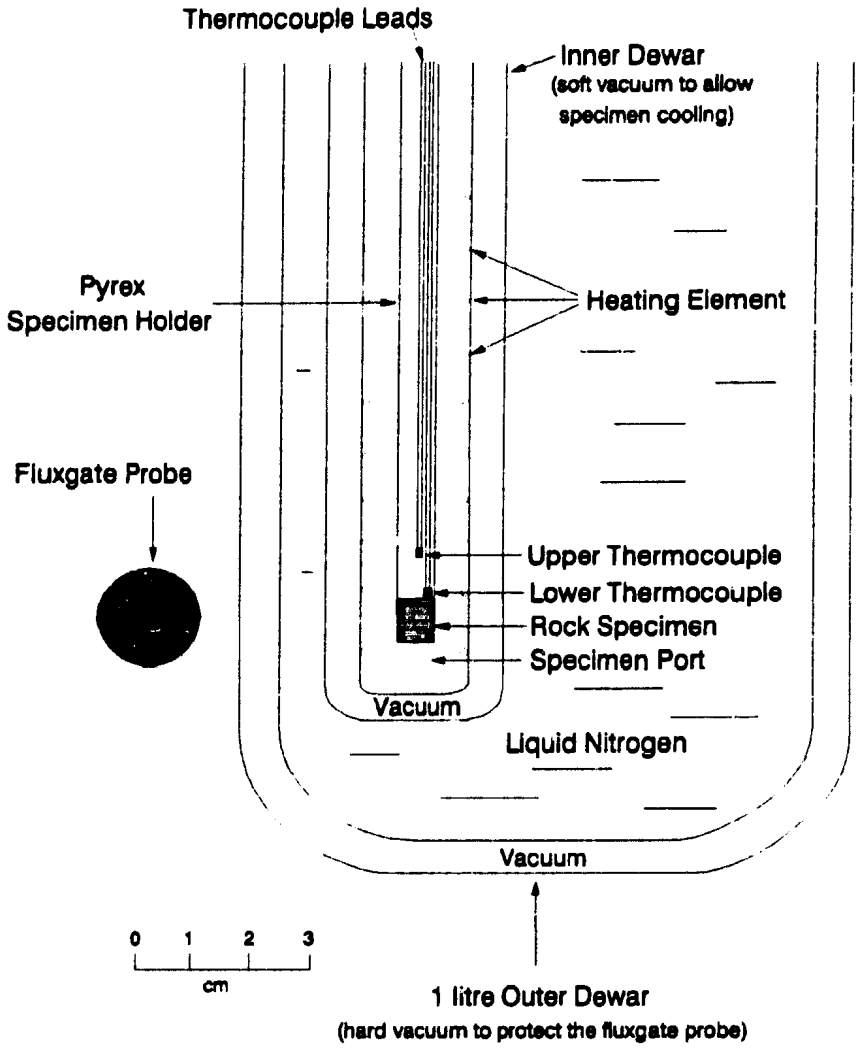

Fig 3.1 Details of Temperature Control Assembly for low temperature demagnetization apparatus

thermocouples). The T-type thermocouple is suitable for these low temperature experiments since it can reliably measure temperatures down to 73 K and is non-magnetic. The positioning of the two thermocouples is illustrated in Figure 3.1. The first thermocouple is in contact with the upper surface of the rock specimen and is used to indicate the temperature of the specimen itself. The second is placed 1 cm (*one specimen length*) above the specimen and is used to give a rough measure of the temperature gradient in the rock specimen. A double pole double throw switch allowed both thermocouples to be read using the same Leeds and Northrup potentiometer (*model 211a*).

3.2 Testing the performance of the apparatus

a.) Sensitivity of the magnetometer on cooling

The response of the fluxgate probe could be temperature-sensitive. Hence we tested whether its sensitivity remains constant as the specimen port is cooled. To do this we substituted a small solenoid with a known current through it for the specimen's magnetization. The solenoid was positioned near the fluxgate element outside the 1 litre Dewar. Current to the solenoid was supplied by a Kepco power supply (*model TQE 25-4*). At particular current settings, a specific magnetic moment was generated by the solenoid causing a deflection on the magnetometer meter. At room temperature in the specimen port, current of 25, 50, 75, 100, 125 and 150 mA was supplied to the solenoid and the corresponding magnetometer readings were recorded. This was repeated at progressively lower temperatures in the specimen port (measured 1 cm above the bottom

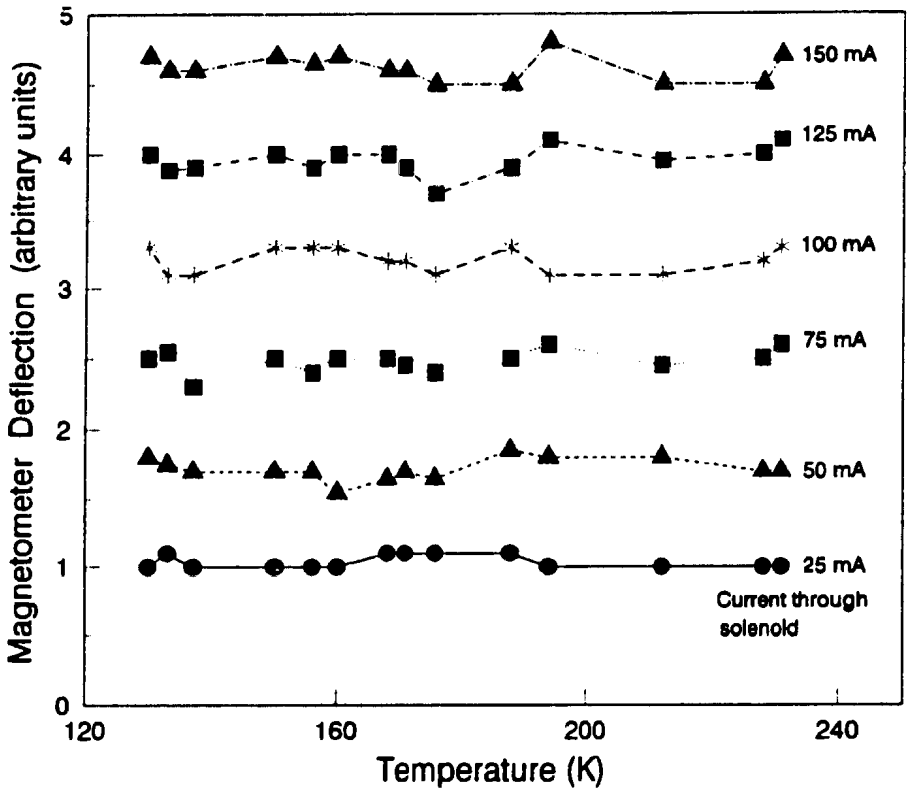

Fig 3.2 Sensitivity of the magnetometer as a function of temperature in specimen port

of the port). Figure 3.2 illustrates how the magnetometer readings for a given current to the solenoid remained constant on cooling, thus indicating that the fluxgate element's sensitivity is independent of the temperature in the specimen port. The slight fluctuations probably represent fluctuations of the Earth's magnetic field some of which penetrate the magnetic shield. Because these fluctuations are slight (corresponding to $\pm$ .15 Am^{-1} in magnetization change) they do not cause serious errors ($< 5\%$) in the magnetization measurements made.

b.) Temperature gradient testing

Since the inner Dewar is open to room temperature at one end, a temperature gradient along the length of the Dewar is expected. This temperature gradient is expected to vary with the amount of current through the heating element. The temperature gradient for various current settings to the heating element was determined to select a position for the rock specimen such that the temperature gradient would not be excessive regardless of the current setting.

For a specific current setting to the heating element, a T-type thermocouple was placed at the bottom of the inner Dewar and the temperature was recorded. Then the thermocouple was repositioned 1 cm above the bottom, and again the temperature was recorded. This procedure was repeated until a height of 7 cm above the bottom was reached. To ensure thermal equilibrium, the thermocouple was left 30 minutes at each position before measuring the temperature.

Figure 3.3 shows the resulting temperature profiles for current settings to the

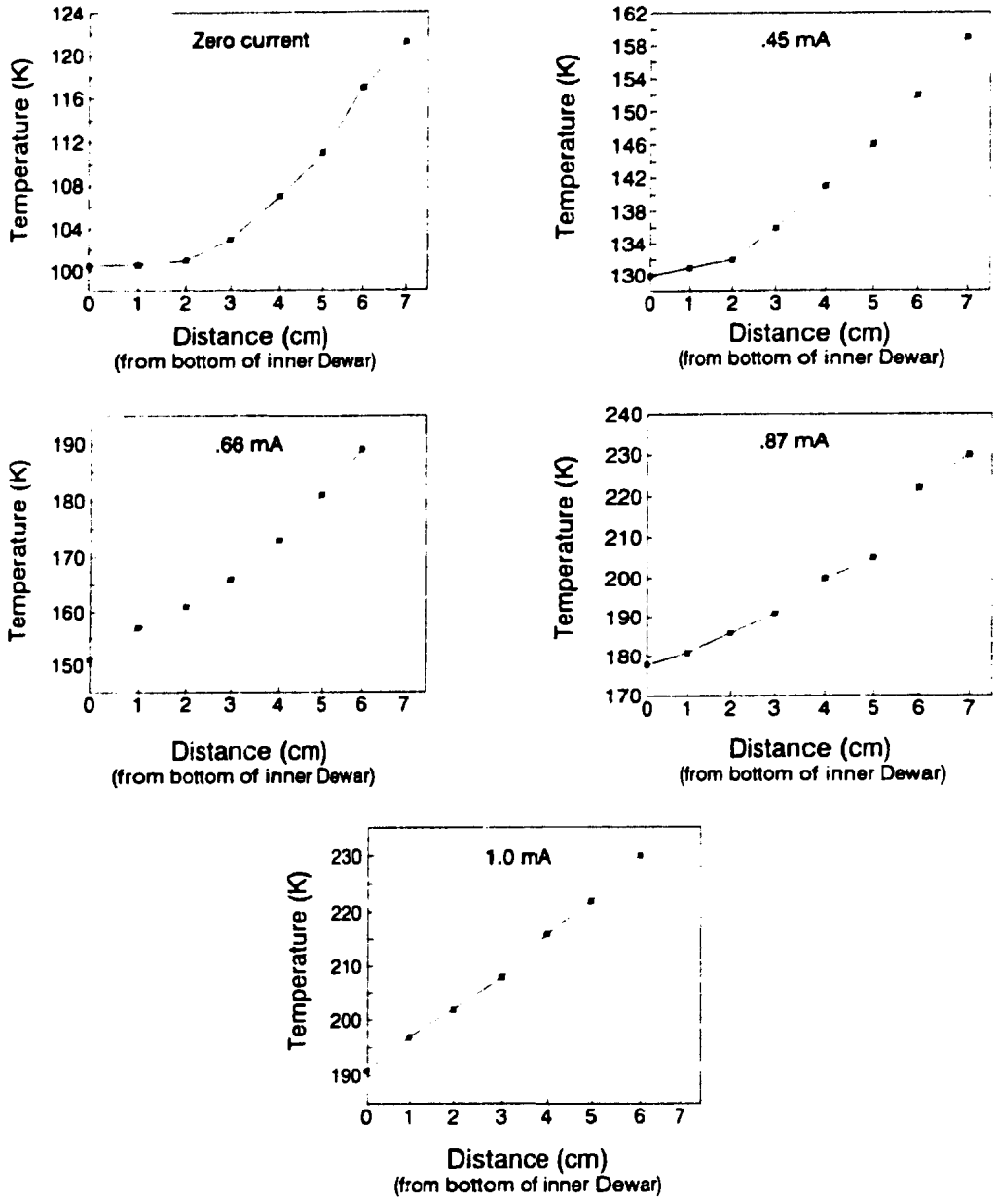

Fig 3.3 Temperature profile in the inner Dewar using various heating coil currents

heating element of 0, .45, .66, .87 and 1.0 mA. A specimen position between 1 and 2 cm from the bottom was chosen since this gives about the lowest temperature gradient and allows the rock specimen to rotate unobstructed. As shown in Figure 3.3a and b, with 0 and .45 mA passed through the heating element, the temperature gradient between 1 and 2 cm seems to be slight (*only about .4° and 1° per cm respectively*). Figures 3.3c, d and e show that for .66, .87 and 1.0 mA passed through the heating element, the temperature gradient between 1 and 2 cm increases to 4°, 5° and 6° K per cm. Hence the rock specimen was positioned between 1 and 2 ms above the bottom of the inner Dewar for all experiments. The temperature gradient should be small especially at temperatures lower than 150 K (*Figures 3.3a,b and c*) and thus little smearing of important magnetic transitions is expected. At higher temperatures the gradient is larger, but the magnetization change with temperature is more gradual making this tolerable.

c.) Estimation of errors

As described in *Section 3.1*, two thermocouples were positioned inside the inner Dewar. The lower thermocouple touching the top of the specimen is used to indicate the temperature of the rock specimen itself while the other thermocouple measures the temperature 1 cm above. The difference between these two temperatures gives a rough estimate of temperature difference across the rock specimen. At each measurement of magnetic intensity, the sample's temperature was recorded from the lower thermocouple and its error was estimated as the difference between the temperature read from the lower and upper thermocouples. As seen in the graphs of Figure 3.3 this should give a

reasonable estimate of the error in temperature for the rock specimen and may indeed overestimate error at temperatures less than about 130 K.

Magnetization intensity was measured by rotating the specimen 180° and recording the change in field at the fluxgate element. This field change is proportional to magnetization and was calibrated by measuring the initial room temperature remanence intensity with a Schonstedt spinner magnetometer (*model SSM-1*). The error in measurement of the magnetization intensity on cooling seems mainly due to noise from fluctuations in the Earth's magnetic field during the measuring. The percent error depends upon the intensity of magnetization and varies from 1% for the strongest remanence (234 Am^{-1} for SIRM of specimen 3203) to 6% for the weakest remanences (.91 Am^{-1} for NRM of specimen 3203).

d.) Procedure for measurement of magnetization intensity

The specimen is given a remanence whose intensity is measured on the Schonstedt spinner magnetometer. The 1 litre Dewar is kept filled with liquid nitrogen and current is applied to the heating element and adjusted to get near room temperature in the specimen port. The specimen is placed in the specimen port (*Figure 3.4*) and is rotated for maximum field at the fluxgate probe. The specimen is then rotated 180° with respect to the fluxgate probe and the fluxgate probe meter deflection is recorded. This reading is proportional to the specimen's magnetization whose absolute value was measured on the spinner magnetometer and is used to calibrate the fluxgate probe readings.

The specimen's magnetization change with temperature is then monitored by

measuring the fluxgate probe meter deflection on rotating the specimen 180° for various temperatures. Before each measurement, the specimen is allowed to come to thermal equilibrium which takes 30 to 40 minutes.

Figure 3.4: Photo of the dial and pyrex shaft being inserted in the specimen port.

Chapter Four

Experimental Results

4.1 Selection of Rock Specimens

Dolerite block samples were collected (*by K.L. Buchan and J.P. Hodych*) near Nain, Labrador, at 39 sites in a dyke swarm with a U-Pb baddeleyite age of 1,277±3 Ma (*J.C. Roddick*, personal communication, 1994). To determine the paleomagnetic viability of these dolerites, one cylindrical specimen (2.5 cm height, 2.5 cm diameter) from each site had been step-wise AF-demagnetized (I did about 20% of these demagnetizations). Demagnetization was done along three perpendicular axes with a Schonstedt AF-demagnetizer (*model GSD-1*) using 5 mT steps between 0 to 20 mT, and 10 mT steps between 20 to 100 mT. After each AF-demagnetization step, the residual moment was measured on the Schonstedt spinner magnetometer.

Of the initial 39 specimens, 21 carried a stable *westerly* direction of remanence, and 12 of these stable specimens had AF-demagnetization curves exhibiting quadratic decay behaviour (Figure 4.0d shows a good example). An AF-demagnetization curve with a square or quadratic shape is usually considered to be characteristic of a stable remanence held in single-domain (SD) or pseudo-single domain (PSD) magnetite grains [*Lowrie and Fuller*, 1971; *Dunlop et al.*, 1973; *Dunlop and Argyle*, 1991]. In contrast, an AF-demagnetization curve showing an exponential decay is considered to be characteristic of remanence held in multidomain (MD) grains [*Evans and McElhinny*, 1969; *Heider et al.*, 1988].

Figures 4.0d to 4.11d show the AF-demagnetization curves of natural remanent magnetization (NRM) for the 12 specimens chosen for this thesis. They all show quadratic decay, and many have a distinct plateau showing little decrease for the first 10 to 15mT of AF-demagnetization. We assume that NRM in these specimens is likely carried by SD or PSD magnetite grains rather than by large MD magnetite grains.

To help determine what mineral carries the stable NRM in these 12 specimens, companion specimens from the same blocks were thermally demagnetized in steps. A Schonstedt thermal demagnetizer (*model TDS-1*) was used. Temperature steps of 100°C were used between room temperature and 500°C, and then 20°C steps were used beyond 500°C (temperatures being accurate to about $\pm$10°C) until intensity was reduced to less than 10%. The residual moment after each thermal demagnetization step was measured on the Schonstedt spinner magnetometer.

The thermal demagnetization curves are shown in Figures 4.12 and 4.13. Most show that intensity is reduced to about 2%-4% of its initial value within 20°C of 580°C, which is the Curie temperature for magnetite. However, it must be noted that the Curie temperature T_c will be shifted to lower temperatures with increasing Ti content (i.e. magnetite is part of the titanomagnetite series: $Fe_{3-x}Ti_xO_4$, $0 \geq x \geq 1$, where $x=0$ is pure magnetite). One specimen shows that intensity is reduced to less than 5% at 540°C, suggesting that its magnetite may contain about $x=0.1$ molar fraction of Ti^{+4}. Also four other specimens showed a reduction to 2-4% at 560°C, indicating a possible molar fraction $x = 0.04$ of Ti^{+4}.

4.2 Results of low-temperature demagnetization

Three types of remanence were measured on cooling to 93 K, and then warming back to room temperature for this thesis: natural remanent magnetization (NRM), anhysteretic remanent magnetization (ARM) and saturation isothermal remanent magnetization (SIRM). The NRM cooling had to be done first since NRM cannot be produced in the laboratory whereas the artificial remanences ARM and SIRM can be.

The rock specimens for low-temperature demagnetization were ground into cylindrical cores 1 cm in height and .9 cm in diameter. They were cut so that the NRM direction was roughly perpendicular to the cylindrical axis to maximize the magnetometer deflection.

Remanence intensity was usually measured at 10° or 15° temperature increments from room temperature to about 140 K. Between 140 K and 93 K the temperature increment was reduced to 5° since intensity may dramatically change around the magnetocrystalline isotropic point ($\approx$130 K) or the Verwey transition ($\approx$120 K). Intensity was measured on warming back to room temperature using the same temperature increments as used on cooling. The low-temperature demagnetization results for NRM are shown in Figures 4.0a to 4.11a.

After low-temperature demagnetization of NRM, the specimen was given an ARM. First the specimen was demagnetized at a peak alternating field of 100 mT along three perpendicular axes to erase any remaining NRM. Then, ARM was given to the specimen by superimposing a peak alternating field of 70 mT on a small direct field of

0.2 mT and reducing the AF field slowly to zero. This was done with a Schonstedt AF demagnetizer (*model GSD-1*), whose AF coil had an extra layer of windings added to produce the 0.2mT direct field. ARM was given perpendicular to the specimen's cylindrical axis. The low-temperature demagnetization results for ARM are shown in Figures 4.0b to 4.11b.

After low-temperature demagnetization of NRM and then ARM, the remaining remanence was AF-demagnetized. Then the specimen was given a saturation remanence at room temperature by being placed between the poles of an electromagnet and having a 350 mT field applied perpendicular to the specimen's cylindrical axis. Low-temperature demagnetization results for SIRM are shown in Figures 4.0c to 4.11c. The results of the low-temperature experiments are summarized in Table 4.1.

4.3 AF-demagnetization of ARM and SIRM

After the low-temperature demagnetization of their ARM, each specimen was again given an ARM which was AF-demagnetized in the same way as the NRM. After low-temperature demagnetization of SIRM, each specimen was demagnetized in a 350 mT peak alternating field while being tumbled about three axes. Then the specimen was again given an SIRM in the 350 mT field of an electromagnet and AF demagnetized in the same way as the NRM.

The AF-demagnetization curves for NRM, ARM and SIRM are shown in Figures 4.0 to 4.11. The median destructive field (MDF) associated with each of these AF-curves is shown in Table 4.0. The MDF represents the AF peak field at which remanence is

demagnetized to one-half its initial value and can be used as a convenient measure of magnetic hardness.

4.4 Effects on recovery of cycling to liquid nitrogen temperature (77 K)

The temperature control assembly can achieve a lowest temperature of 93 K, not reaching 77 K due to the insulating properties of the Dewar and to the Dewar being exposed to room temperature at its open end. Remanence kept decreasing below 120 K in some SIRM and ARM low temperature experiments. This might be due to T_v being shifted to temperatures lower than 120 K or even 93 K by Ti content for example. Hence it was desirable to measure remanence at 77 K and its recovery at room temperature.

Table 4.0 Summary of the *median destructive field* (MDF) results obtained from the AF-demagnetization curves of NRM, ARM and SIRM.

specimen	MDF of NRM	MDF of ARM	MDF of SIRM
2701	30 (mT)	29.5 (mT)	20 (mT)
2901	25	28	19
3101	30	31	23
3201	30	28	21
3203	22	26	18
3301	18	19.5	15
3601	33	30	24
4305	47.5	44	35
4601	34	30	24
4602	39.5	31	23
5601	45	38	30
5901	41	43	32.5

To measure intensity at 77 K, the specimen was given an ARM or SIRM, whose intensity was measured at room temperature in the temperature control assembly. The specimen was then withdrawn and submerged in liquid nitrogen in field free space for 10 minutes. Then the specimen was quickly taken out of the liquid nitrogen and reinserted in the temperature control assembly so that its intensity could be measured before it warmed. The specimen was then left inside the temperature control assembly for 30 minutes until it warmed to room temperature in the field free space. Then its remanence intensity was again measured and when divided by the initial room temperature remanence intensity yielded the recovery.

The results of these experiments are shown in Table 4.2 and by two stars in each of Figure 4.0b, c to Figure 4.11b, c. One of these stars gives the fraction of initial remanence remaining at 77 K. This fraction is almost always close to the fraction remaining at 93 K. This suggests that T_v has been reached by 93 K in most specimens. Possible exceptions are specimens 3203, 3301 and 5601. The other star gives the fraction of initial remanence recovered at room temperature, which, except for specimens 3203, 3301 and 5601, should agree with the fraction of initial remanence recovered at room temperature in cycles to 93 K. Exceptions are the fractions of ARM in specimens 3601 and 4602.

Table 4.1 Summary of values taken from low-temperature demagnetization (LTD) cycles of ARM and SIRM for the specimens listed in Table 4.1. *(as measured from Figs 4.0a,b and c - 4.11a, b and c).*

	ARM			SIRM		
specimen	before LTD	at 103 K	after LTD	before LTD	at 103 K	after LTD
2701	$.252*10^{-2}$	.476	.833	.170 emu	.300	.552
2901	$.250*10^{-2}$	.720	.800	.129 emu	.372	.621
3101	$.414*10^{-2}$	.478	.804	.321 emu	.308	.542
3201	$.225*10^{-2}$	.626	.826	.210 emu	.285	.571
3203	$.330*10^{-2}$	.454	.757	.178 emu	.303	.556
3301	$.650*10^{-2}$	.523	.846	.333 emu	.396	.666
3601	$.660*10^{-2}$	.590	.833	.303 emu	.435	.653
4305	$.240*10^{-2}$	.937	1.00	.455 emu	.831	.887
4601	$.450*10^{-2}$	.555	.755	.301 emu	.402	.571
4602	$.250*10^{-2}$	.560	.940	.345 emu	.406	.662
5601	$.500*10^{-2}$	.620	.960	.402 emu	.738	.858
5901	$.300*10^{-2}$	.900	.966	.177 emu	.730	.870

Table 4.2 Summary of low-temperature demagnetization (LTD) of Anhysteretic remanent magnetisation (ARM) and saturation isothermal remanent magnetisation (SIRM).

	ARM			SIRM		
Specimen	before LTD	at 77 K	after LTD	before LTD	at 77 K	after LTD
2701	$.225*10^{-2}$	.533	.826	.165 emu	.454	.545
2901	$.165*10^{-2}$	.636	.854	.132 emu	.386	.590
3101	$.440*10^{-2}$	.568	.772	.380 emu	.368	.552
3201	$.270*10^{-2}$	.566	.733	.216 emu	.277	.555
3203	$.340*10^{-2}$	.205	.529	.168 emu	.267	.600
3301	$.177*10^{-2}$	.338	.750	.390 emu	.435	.692
3601	$.650*10^{-2}$	.523	.750	.350 emu	.428	.628
4305	$.258*10^{-2}$	.883	.930	.460 emu	.847	.869
4601	$.318*10^{-2}$	.481	.707	.282 emu	.489	.595
4602	$.360*10^{-2}$	.444	.760	.330 emu	.400	.606
5601	$.570*10^{-2}$	.438	.736	.650 emu	.415	.600
5901	$.500*10^{-2}$	.840	.980	.450 emu	.777	.800

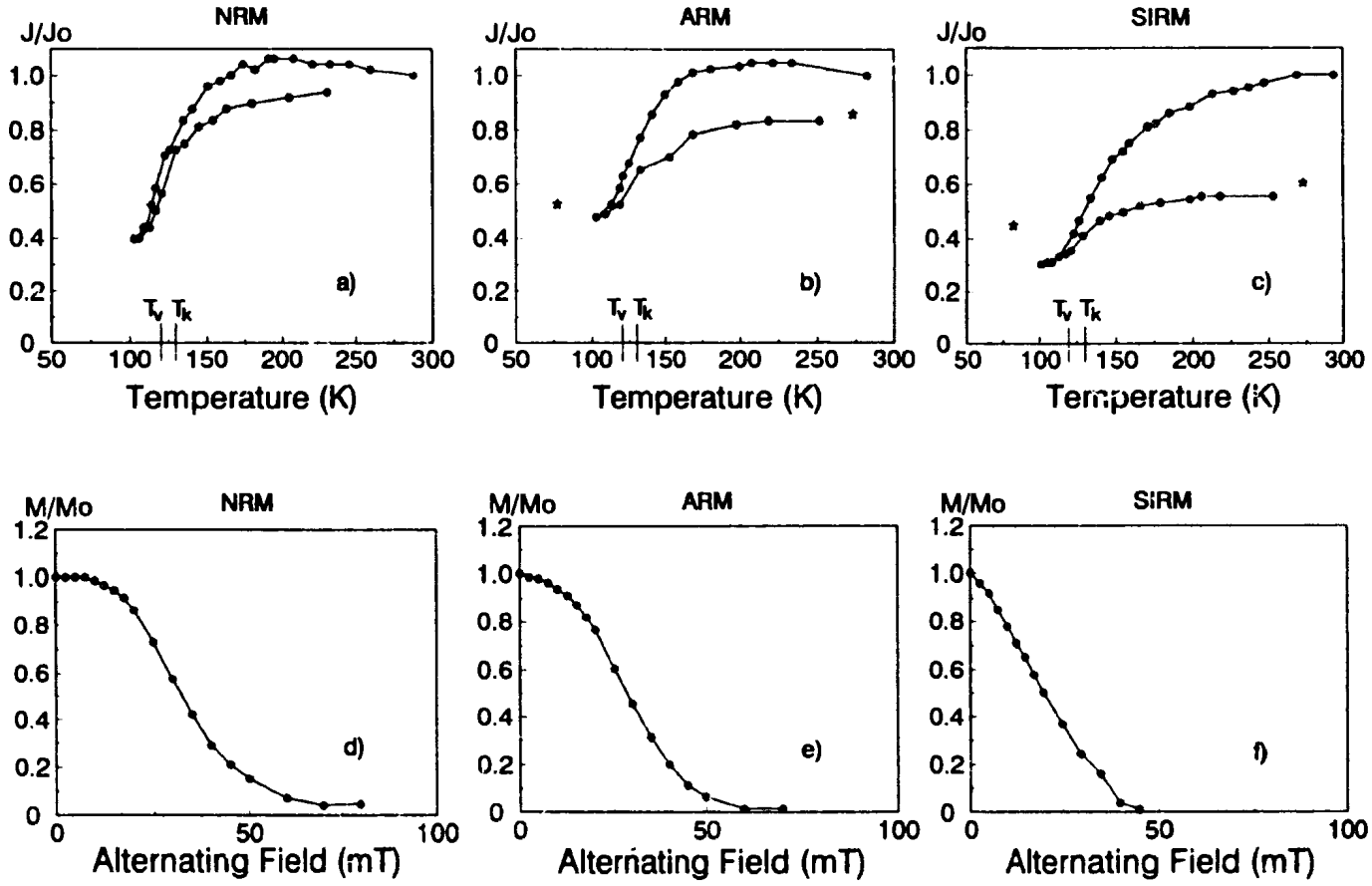

Fig 4.0 Specimen 2701

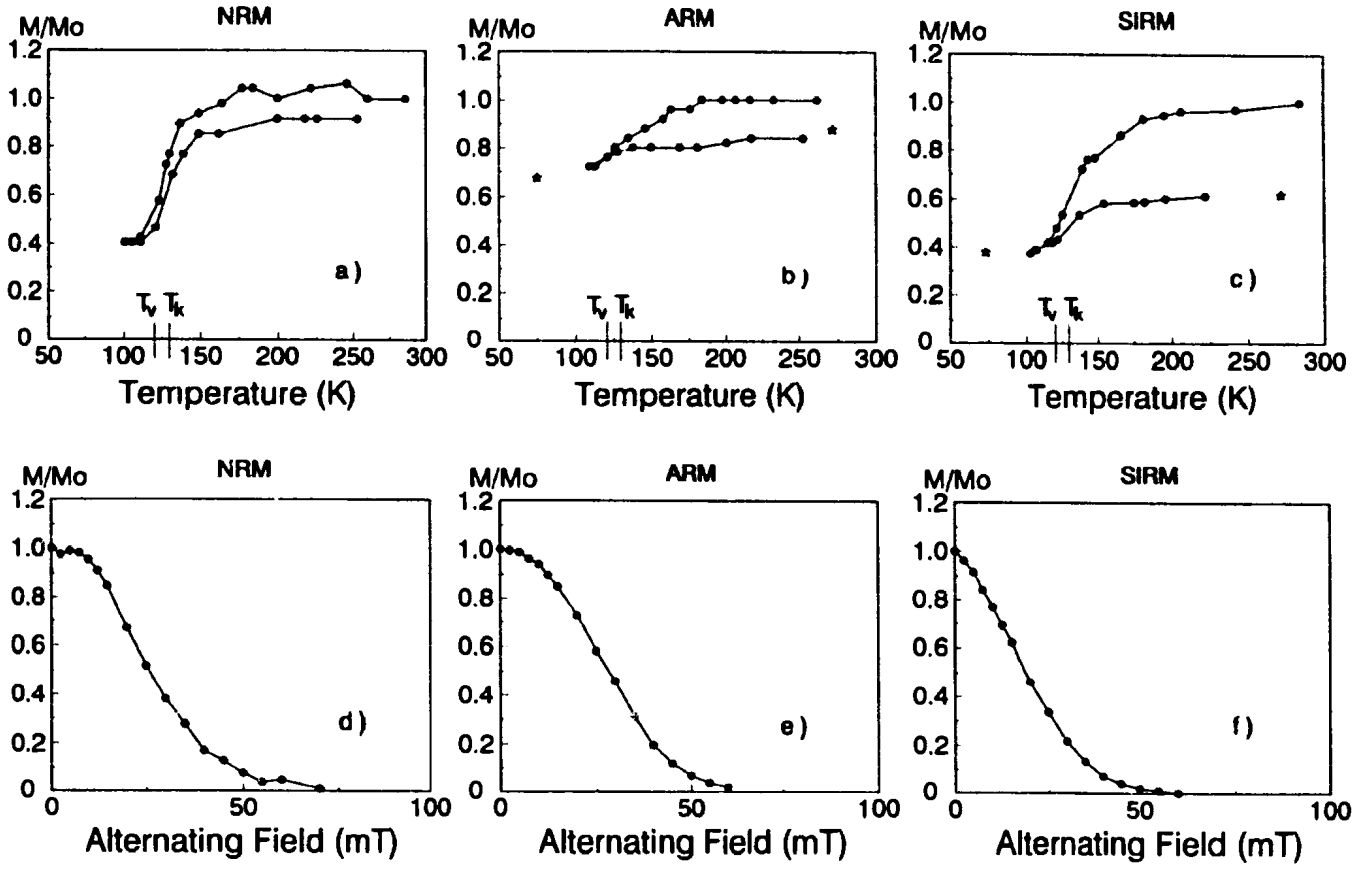

Fig 4.1 Specimen 2901

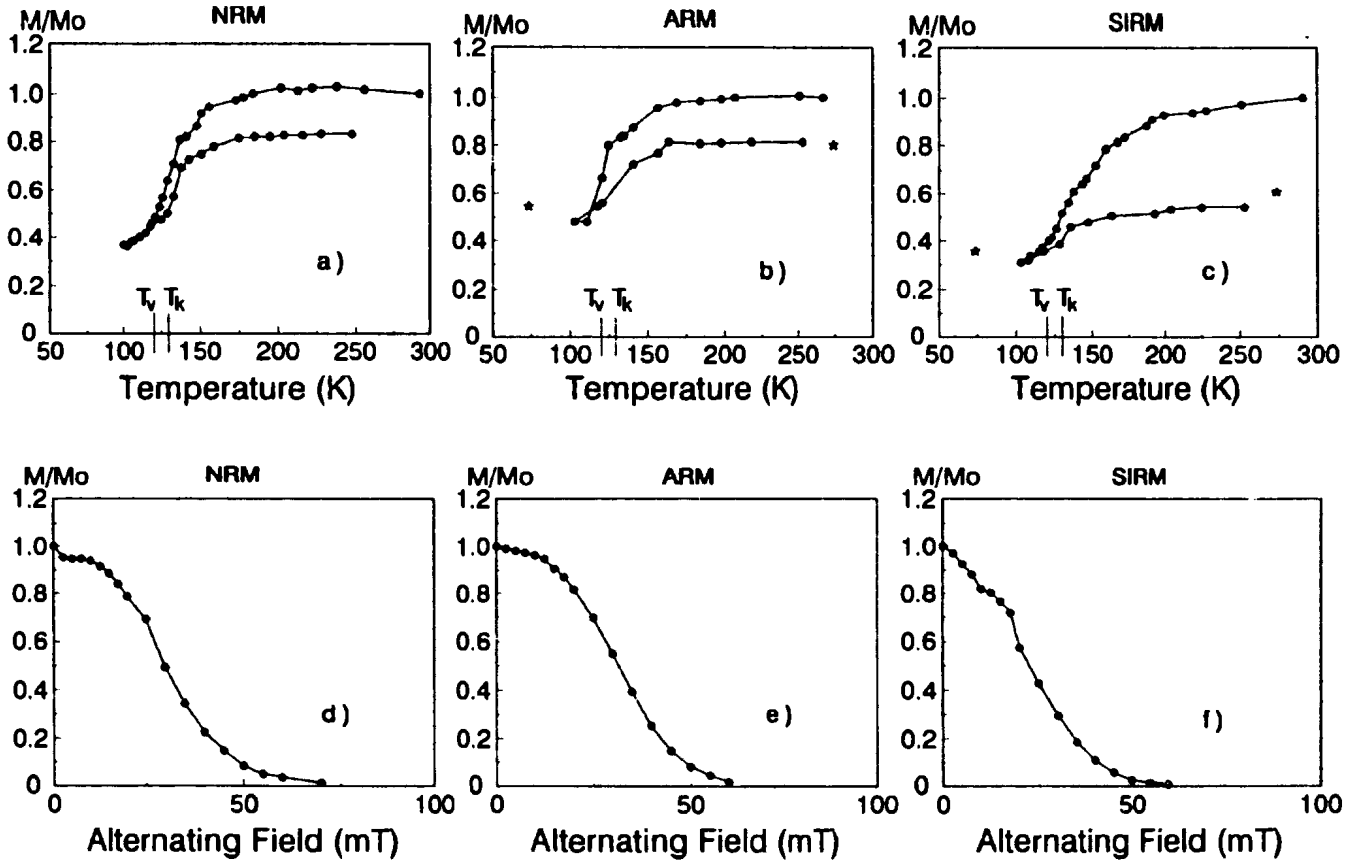

Fig 4.2 Specimen 3101

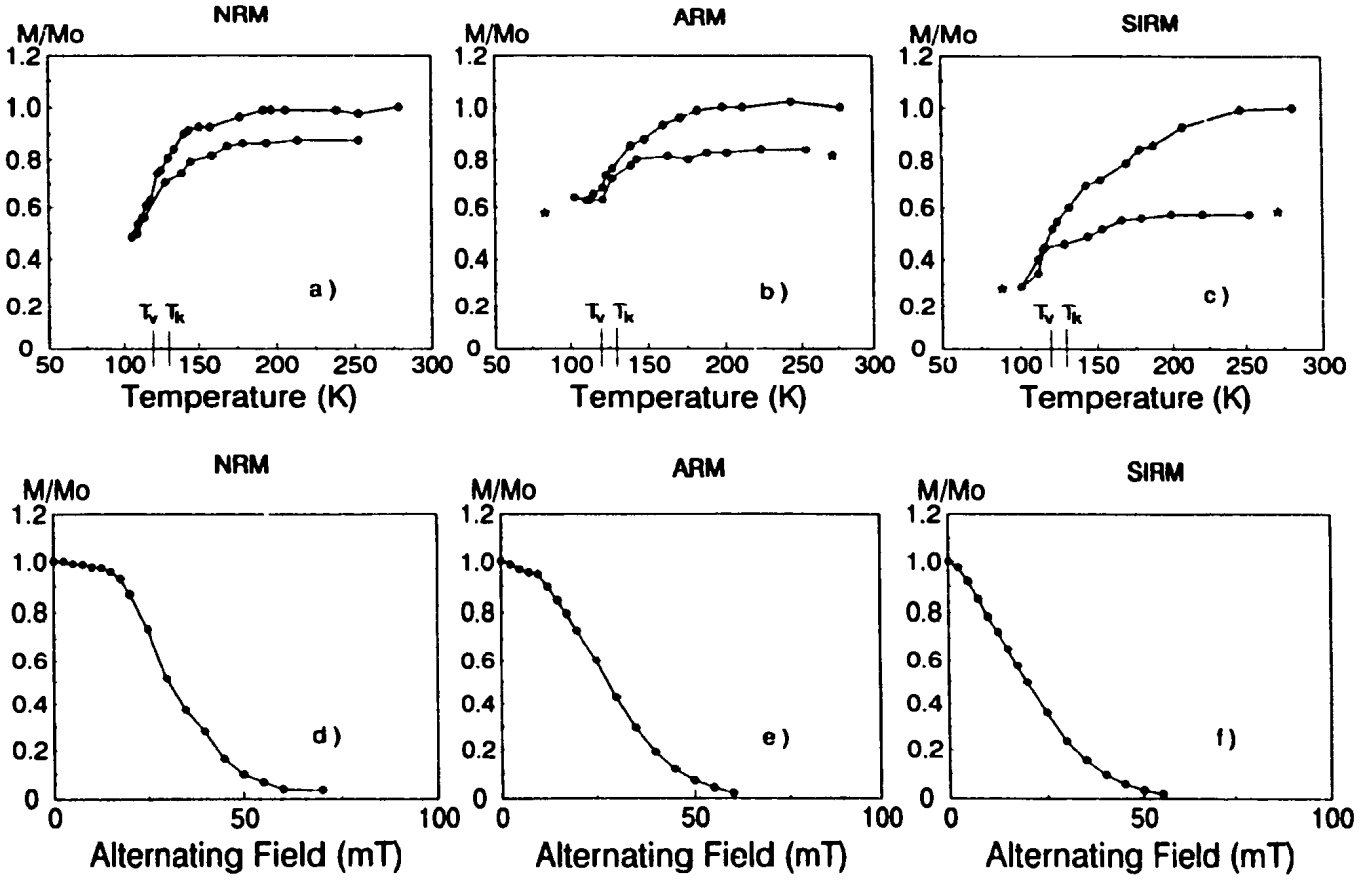

Fig 4.3 Specimen 3201

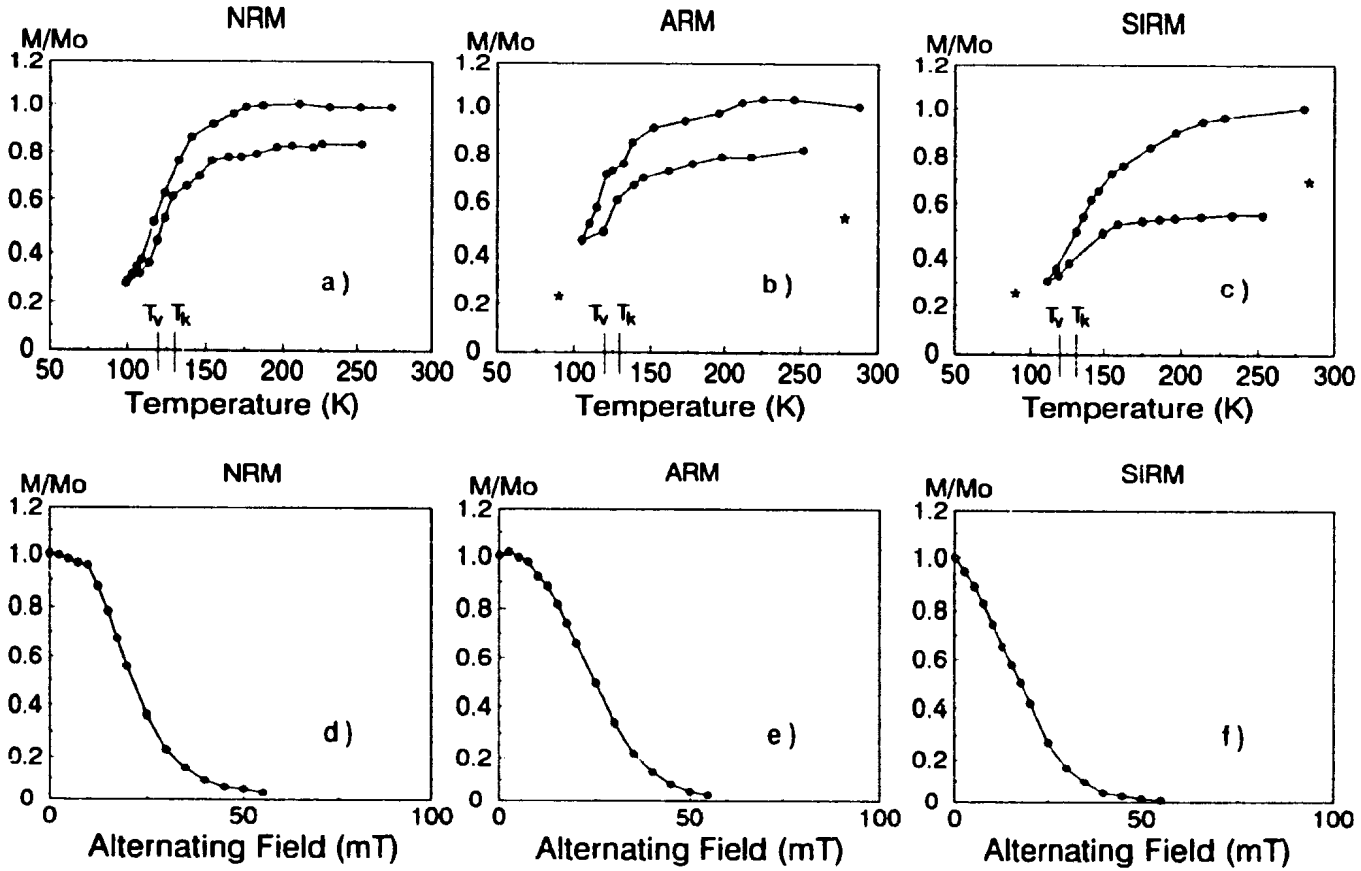

Fig 4.4 Specimen 3203

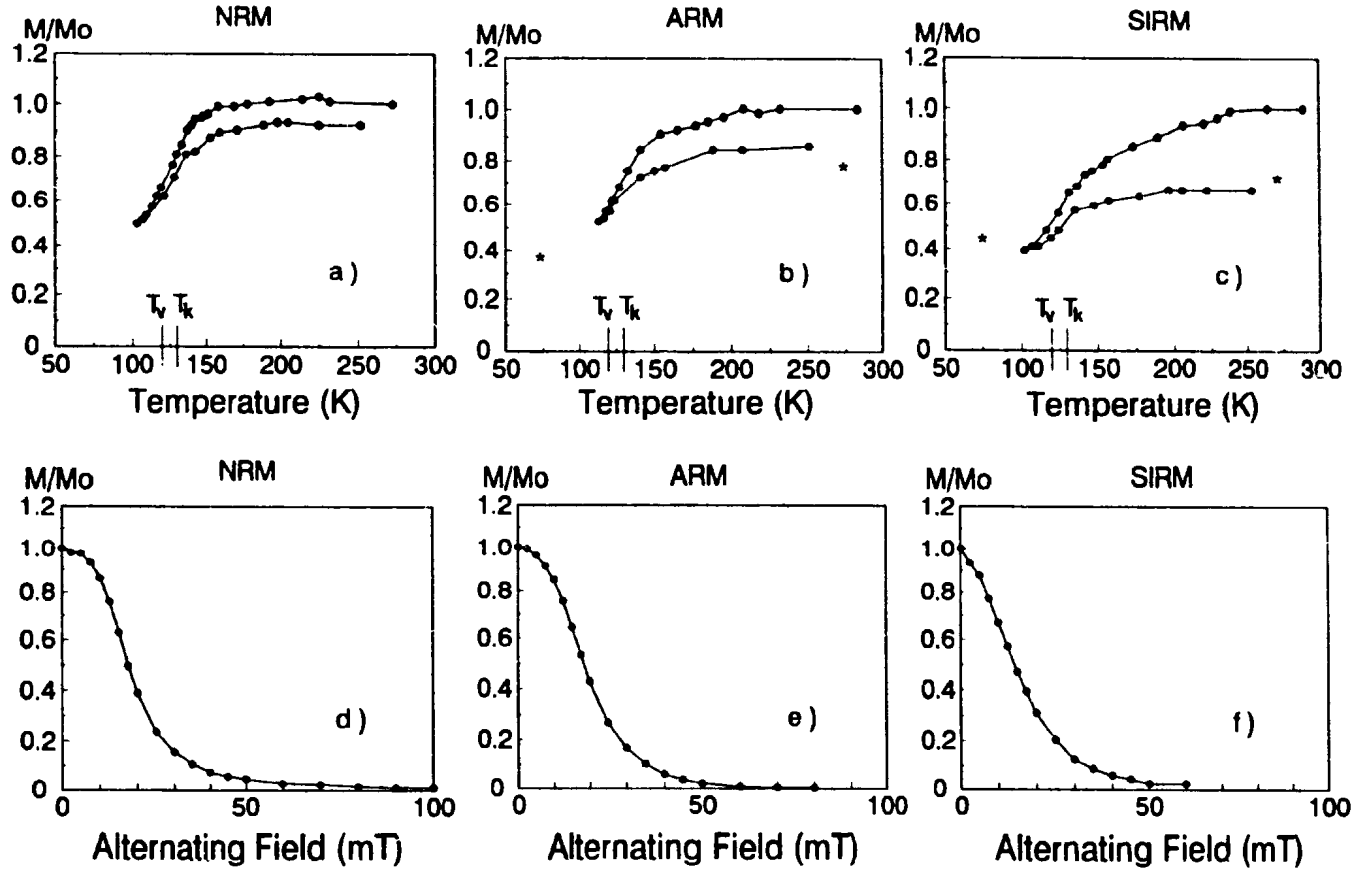

Fig 4.5 Specimen 3301

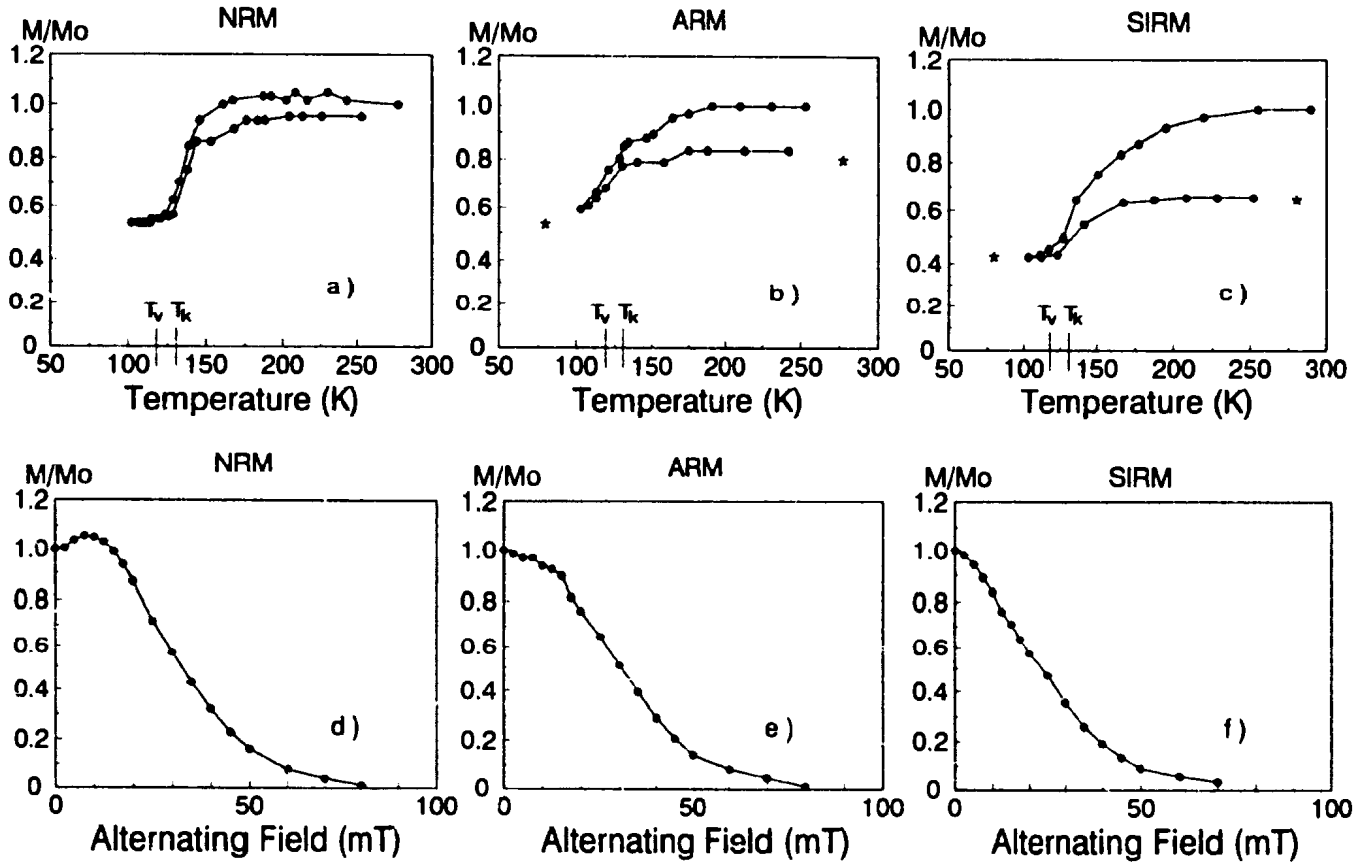

Fig 4.6 Specimen 3601

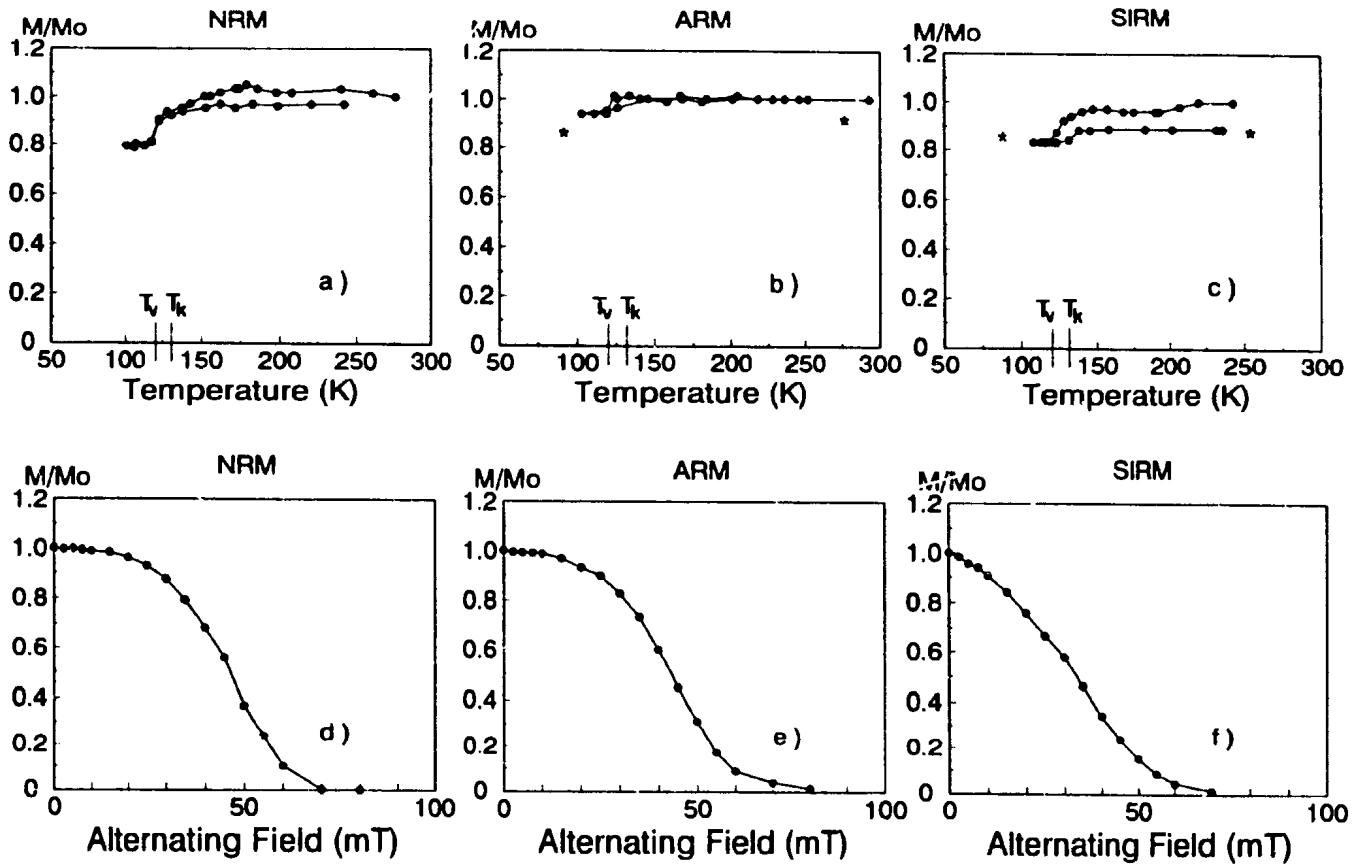

Fig 4.7 Specimen 4305

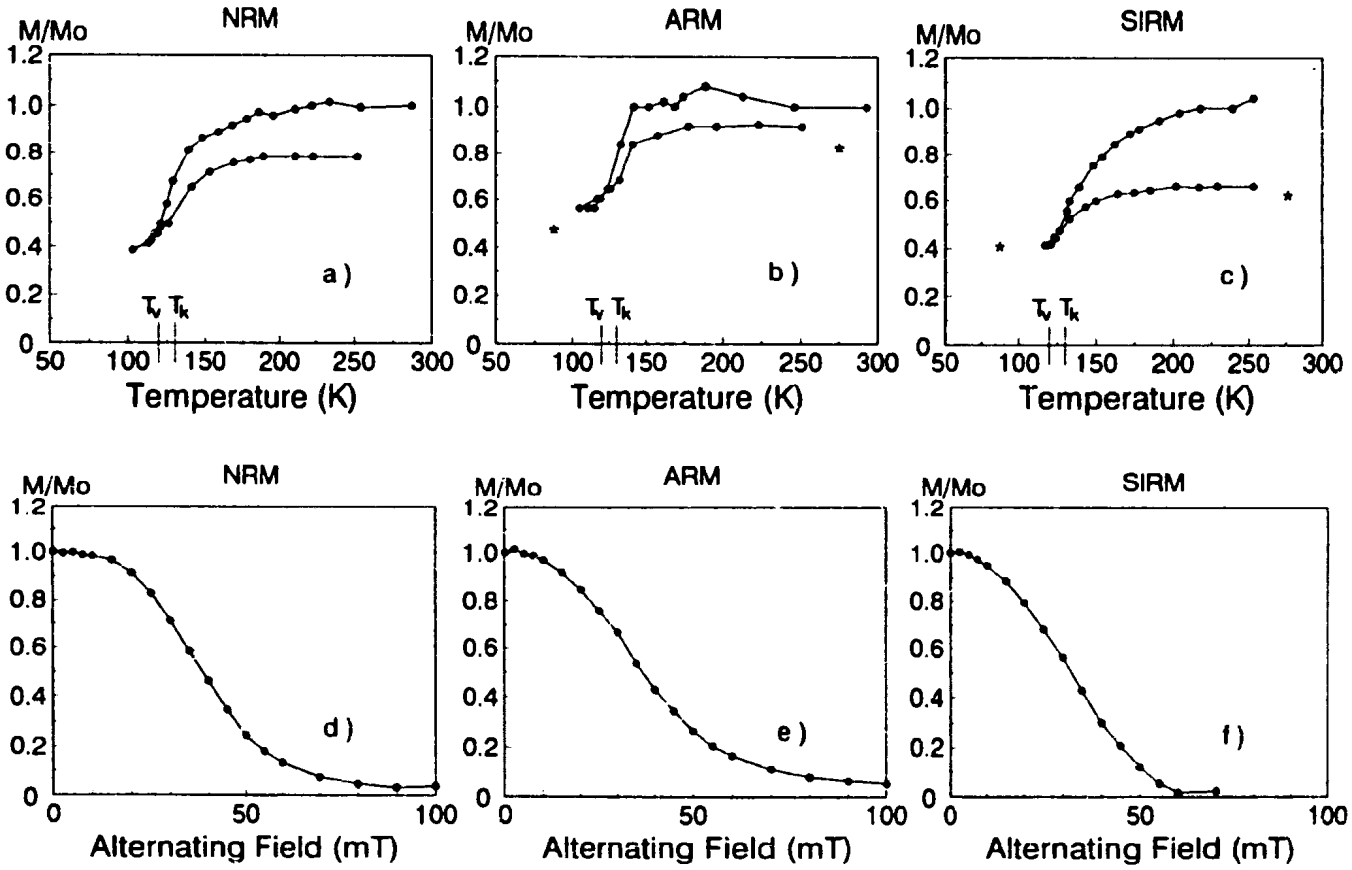

Fig 4.8 Specimen 4602

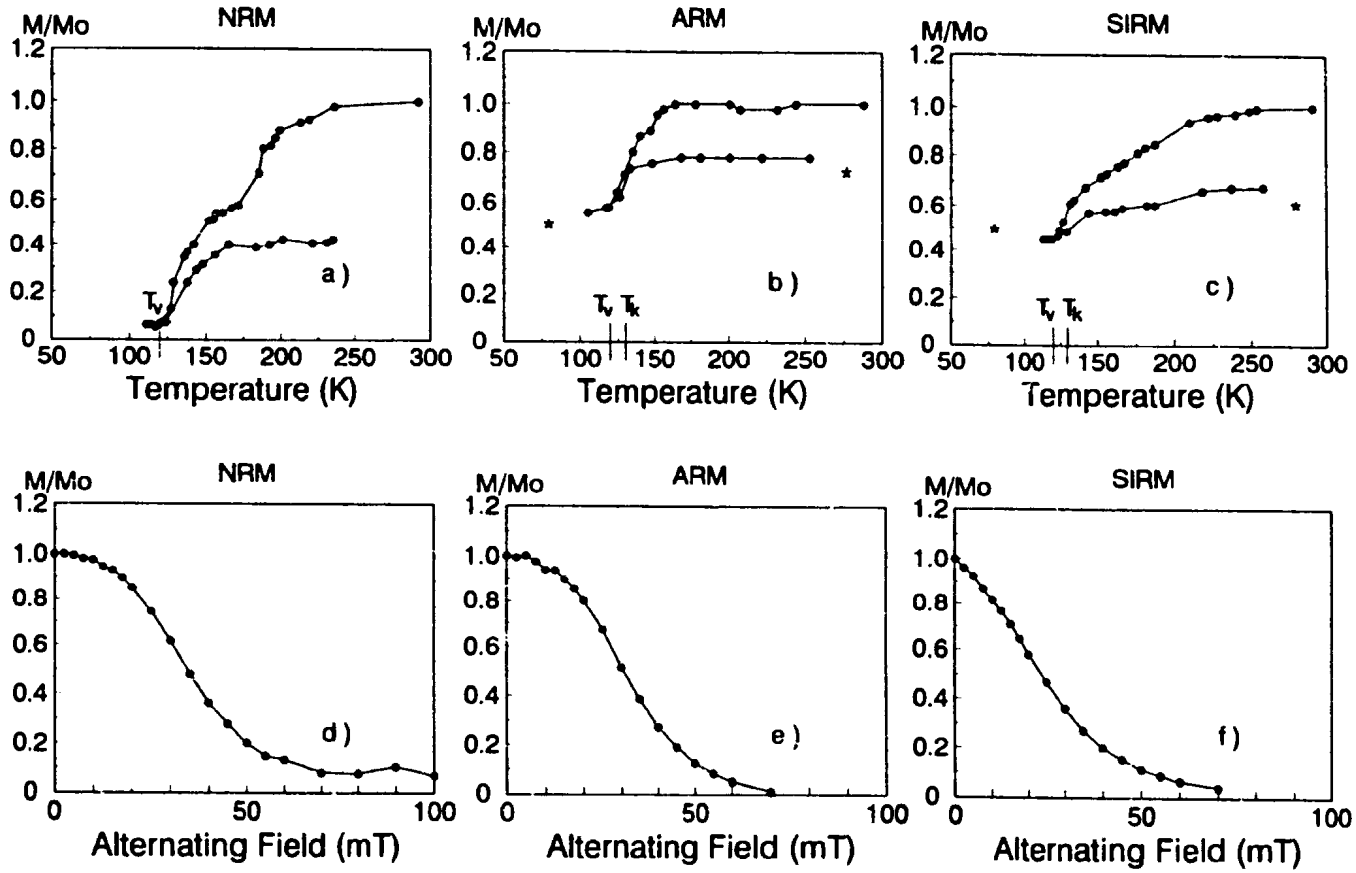

Fig 4.9 Specimen 4601

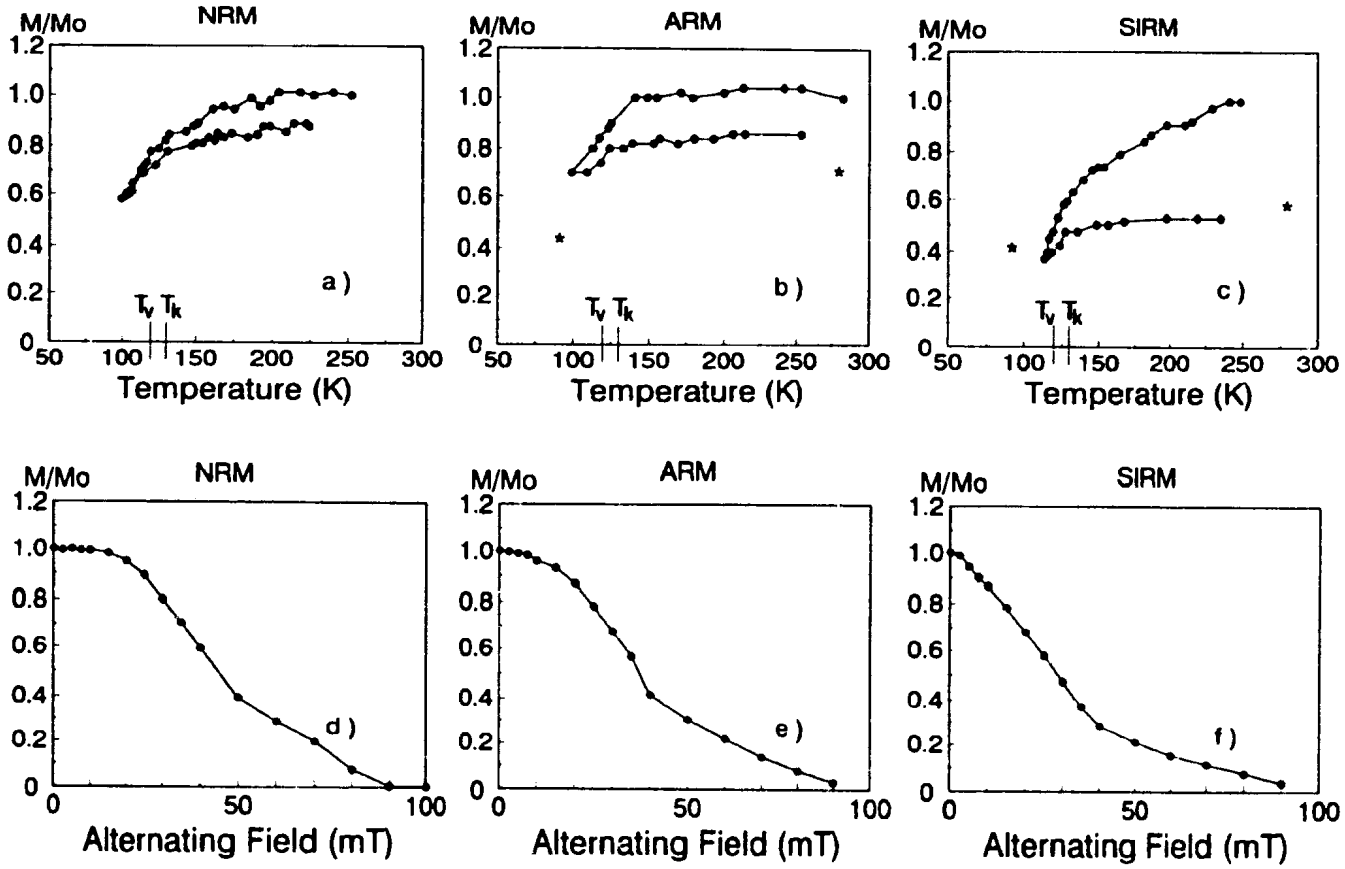

Fig 4.10 Specimen 5601

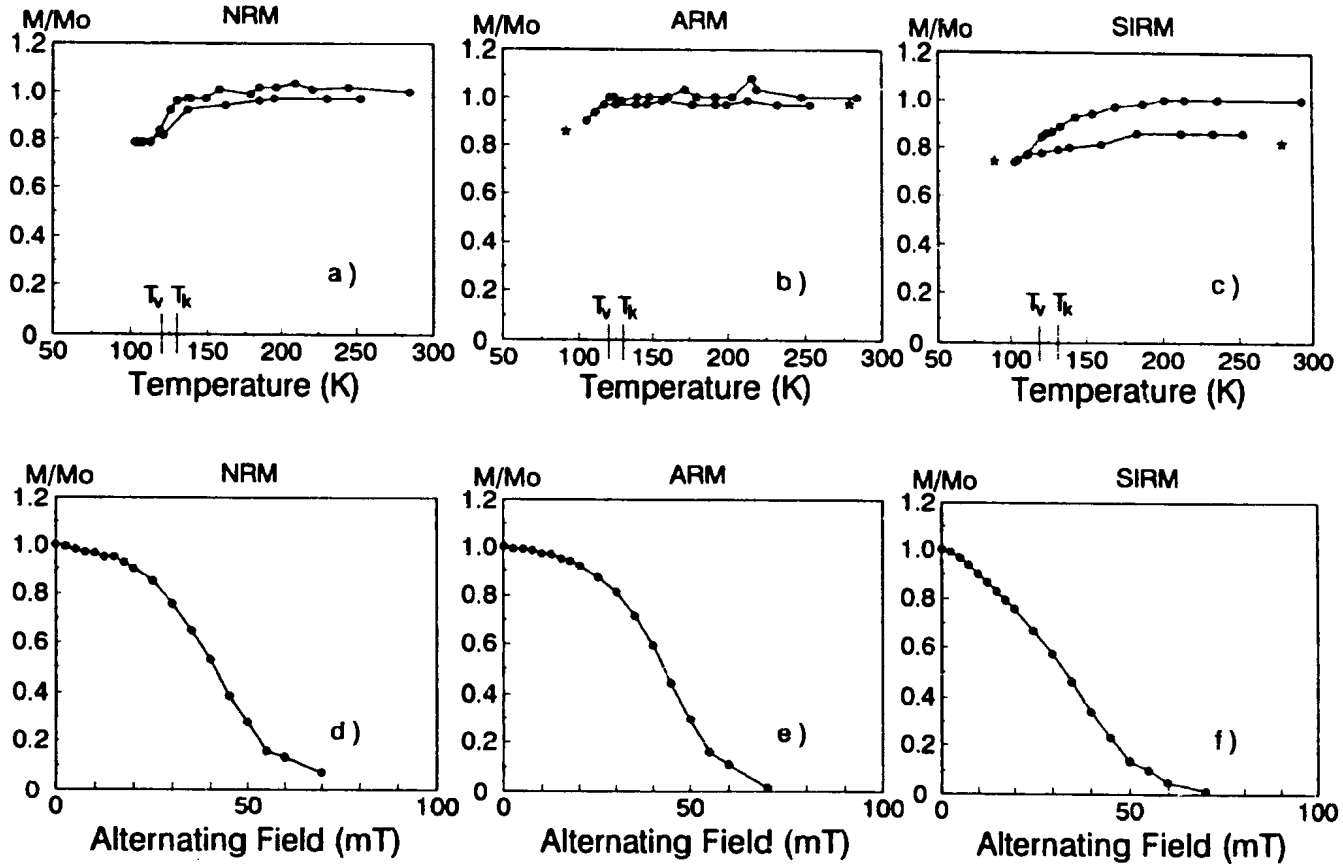

Fig 4.11 Specimen 5901

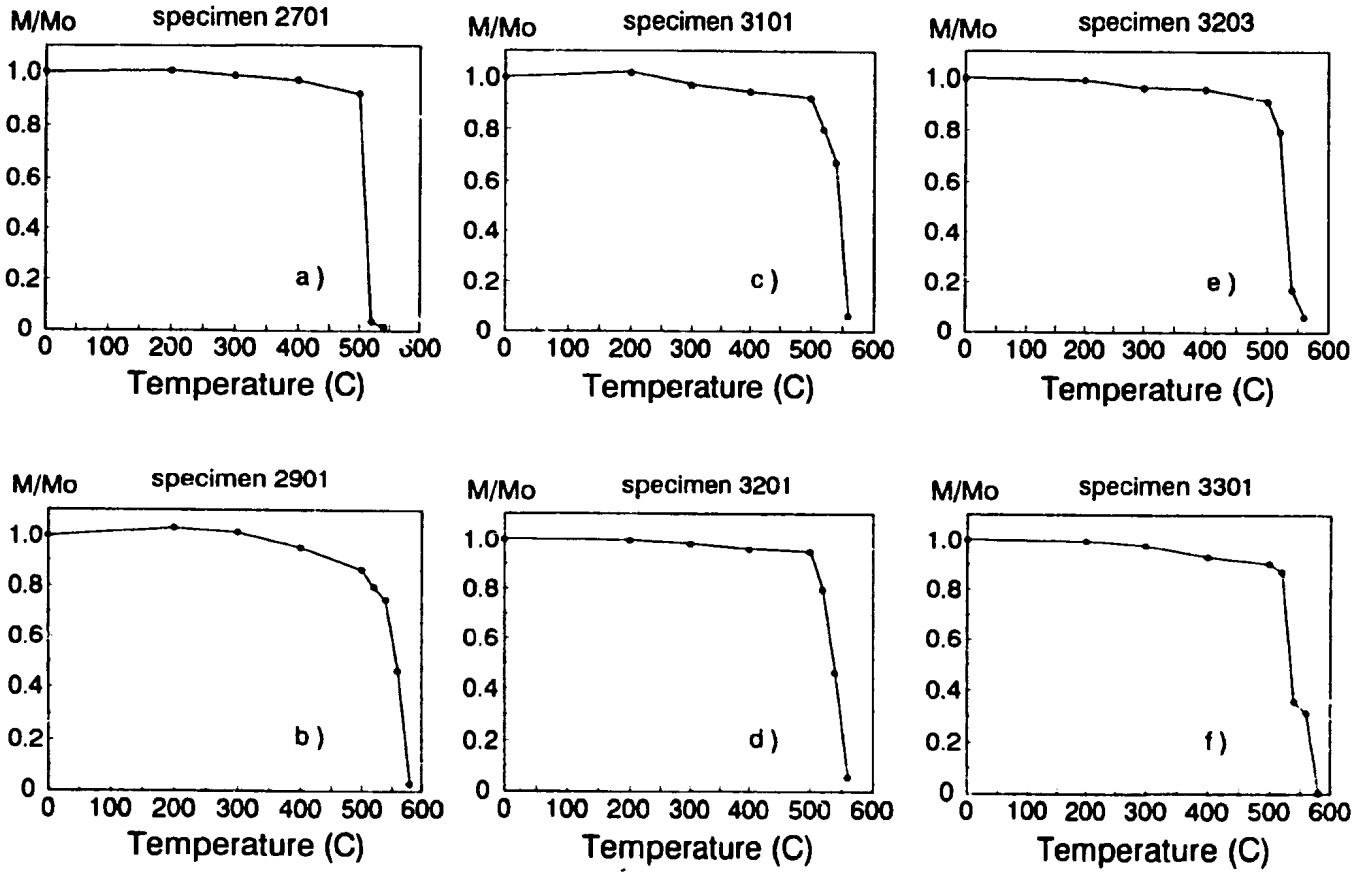

Fig 4.12 Thermal Demagnetization of Paleomagnetic Specimens

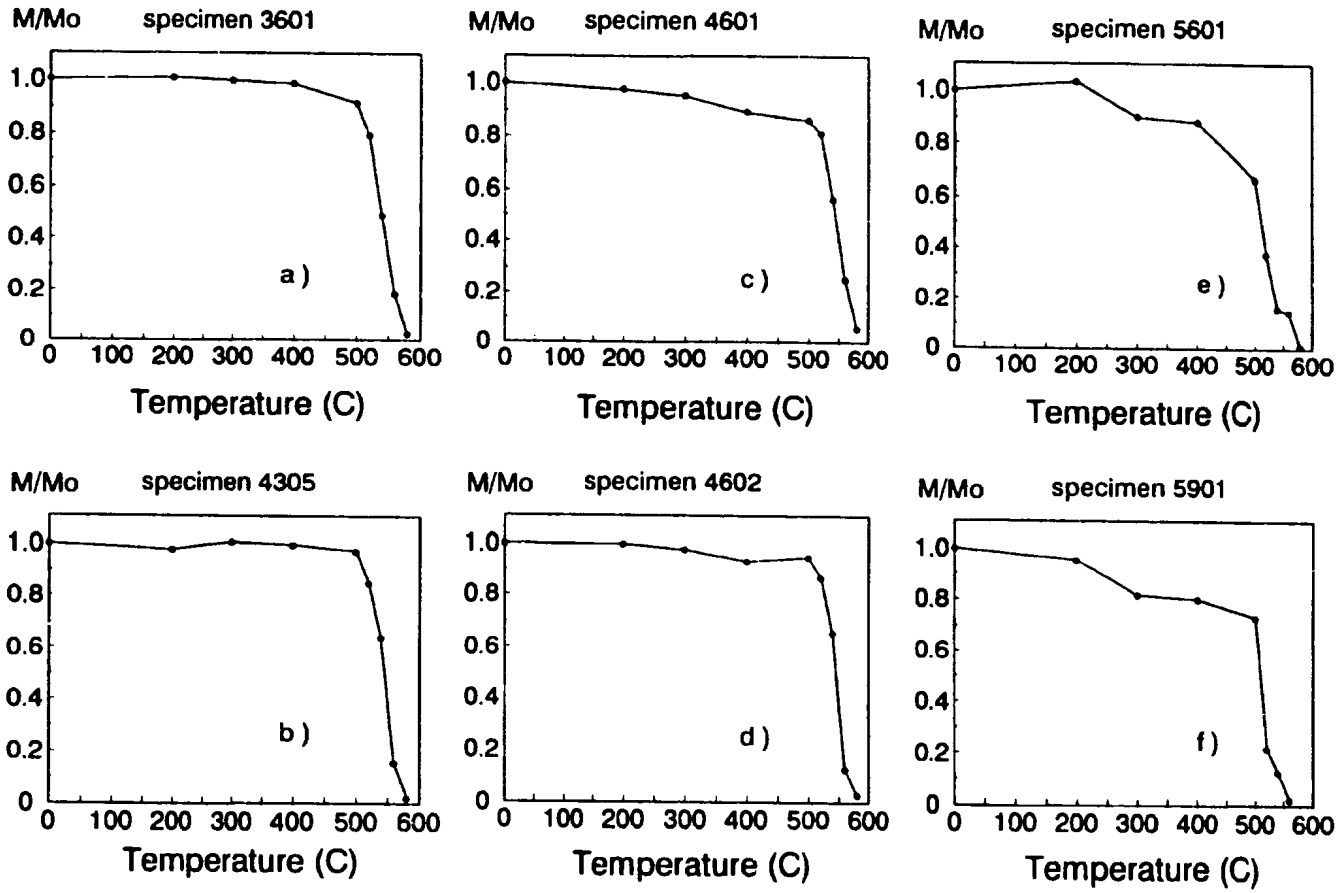

Fig 4.13 Thermal Demagnetization of Paleomagnetic Specimens

Chapter Five

Discussion of Experimental Results & Conclusions

5.0 Magnetic properties of the Nain dolerite dyke specimens

a.) Stability and mineralogy of remanence carrier

The 12 Nain dolerites dyke specimens studied were selected because they showed a stable westerly direction of NRM which is likely primary and because their AF-demagnetization curves exhibited quadratic decay (see Figures 4.0d to 4.11d). Their median destructive fields (MDFs) range from 18mT to 47.5mT, which is high for magnetite-bearing paleomagnetic samples. The shape of these AF-decay curves and the high median destructive fields suggest that stable remanence is held in SD or PSD magnetite grains [*Dunlop and Argyle*, 1991].

To help determine the mineralogy of the remanence carrier of these 12 specimens, thermal demagnetization was done on companion specimens from the same blocks. Curie points of 580 ± 10°C were identified in specimens 2901, 3301, 3601, 4305, 4601, 4602, 5601, and 5901, suggesting pure magnetite. Curie points of 560 ± 10°C were identified in specimens 3101, 3201 and 3203, and 540 ± 10°C in specimen 2701, suggesting magnetite with slight Ti content (560°C suggesting $x\sim0.04$ and 540°C suggesting $x\sim0.07$, as estimated from Figure 2-2a from *Syono* [1965]).

b.) Grain size of remanence carrier

One might hope to make a rough grain size estimate for the remanence carrier by studying the MDFs of the AF-demagnetization curves. According to the conventional

Lowrie-Fuller test [*Lowrie and Fuller*, 1971], the MDF is higher for weak-field TRM than for SIRM if the grains are less than 10 to 15μm in mean diameter whereas the opposite is true if the grains are larger. However, *Heider et al.* [1992] found that the threshold grain size was 100μm, rather than the 15μm estimated by Lowrie and Fuller. We can assume that the largest component of NRM in our specimens is TRM. Hence, a Heider-updated Lowrie-Fuller test can be made by comparing the MDFs of NRM and SIRM in Table 4.0. For all 12 of our specimens, MDF is higher for NRM and ARM than for the corresponding SIRM, suggesting that the magnetite grain size is less than 100μm.

Precise magnetite grain size is very difficult to determine. Commonly in dolerites, the magnetite crystallized as large grains of titanomagnetite (with $x \sim 0.8$) and exsolved on cooling into nearly pure magnetite cut into fine grains by exsolution lamellae of ilmenite. Such fine subdivision by ilmenite lamellae was looked for and found in specimen 4602 using the scanning electron microscope (SEM) in back scatter mode.

5.1 Possible controls on remanence and their expected response to low-temperature demagnetization

There seems to be reasonable agreement that the grain size at which shape anisotropy control of remanence ends and magnetostrictive, or magnetocrystalline control begins in magnetite is about .05μm to 1μm. *Xu and Merrill* [1992] argue from theory that domain walls are magnetostrictively controlled through internal stresses associated with dislocations in grains larger than 1μm, and *Boyd et al.*[1984] argue from Bitter

pattern observations that domain walls cannot nucleate in domains less than 1μm. This suggests that there should not be low-temperature demagnetization through domain wall motion in sub-micron grains, whether the walls are controlled through magnetostriction or magnetocrystalline anisotropy. However *Argyle and Dunlop* [1990] observed a gradual decrease in SIRM held in .540μm magnetite grains on cooling to 100 K; the SIRM decrease was in approximate proportion to the gradual decrease of λ_s on cooling, which suggests magnetostrictive control of domain walls. But remanence in their .215μm and .390μm magnetite was scarcely affected by cooling, suggesting shape anisotropy control. Hence, shape anisotropy control of remanence seems to begin in these specimens just below 0.5μm. We shall not attempt to measure grain size because of the difficulties discussed in *Section 5.0b* but will concentrate on using our low-temperature experiments to determine whether stable remanence is dominantly held through shape anisotropy, magnetostrictive control or magnetocrystalline control.

5.2 Specimens whose low-temperature behaviour suggests shape anisotropy control of remanence

Specimens 4305, 5601 and 5901 all had demagnetization curves for NRM and ARM with quadratic shapes (see Figures 4.7, 4.10 and 4.11) and they had the highest median destructive fields of the 12 specimens studied - 47.5mT, 45mT and 41mT respectively for NRM. Their high median destructive fields and Curie points of 580°$\pm$10°C suggest that the remanence is likely carried by nearly pure SD or PSD magnetite.

Specimens 4305 and 5901 showed little change in NRM and ARM on cooling to 130 K from room temperature but a small decrease in remanence was evident between 125 and 115 K, and further cooling resulted in no further change in remanence. On warming back to room temperature, remanence began to recover just after passing 120 K, and recovery was almost total at room temperature. The corresponding low-temperature behaviour for SIRM was similar, except that recovery of SIRM is a little less than that of the corresponding NRM and ARM which is consistent with the lower median destructive field of SIRM.

The low-temperature behaviour of specimens 4305 and 5901 is what would be expected of SD or small PSD magnetite grains. Coercivity would seem to be controlled by shape anisotropy of the grains, explaining the absence of remanence intensity change from room temperature to near the Verwey transition. The behaviour is like that of the .215μm and .390μm synthetic magnetite of *Argyle and Dunlop* [1990]. Specimens 4305 and 5901 show a small decrease in remanence near the Verwey transition and recovery is nearly complete on warming back to room temperature. The .037μm - .22μm synthetic magnetite of *Heider et al.*[1992] also show nearly complete recovery.

Specimen 5601 also had a Curie point of 580$\pm$10°C suggesting pure magnetite. However, ARM decrease on cooling to 77 K was significantly lower than on cooling to 93 K suggesting that T_v may be depressed below the 120 K for pure magnetite perhaps by oxidation [*Özdemir et al.*, 1993]. The NRM and ARM decrease on cooling resembles the low-temperature behaviour of the 0.540μm magnetite of *Argyle and Dunlop* [1990].

The recovery of SIRM (0.50) after low-temperature cycling was less than the recovery of NRM and ARM (*0.85 and 0.80 respectively*). This suggests that a substantial MD-like component contributes to the SIRM.

5.3 Low-temperature behaviour of the rest of the specimens

a.) General behaviour

Apart from the three specimens of highest MDF discussed above, the rest of the specimens (MDF of NRM ranging from 18mT to 39.5 mT) have similar low-temperature behaviour (Figures 4.0 to 4.6, 4.8 and 4.9). The remanence at first shows a gradual decrease in intensity on cooling from room temperature in zero field. This is followed by a rapid decrease in intensity usually beginning at 125 K to 120 K and ending at about 110 K to 105 K, at which, on average, about 0.55 of initial NRM and ARM, and about 0.35 of initial SIRM remains. Further cooling usually results in little further change in remanence intensity. On warming back, there is at first little change in remanence until an average temperature of about 115 K is reached, when rapid increase in remanence begins. This rapid increase slows at about 130 K to 140 K. Finally at room temperature remanence is, on average, about 0.80 of initial NRM and ARM, and about 0.55 of initial SIRM.

The low-temperature behaviour of NRM, ARM and SIRM are compared for a typical specimen (3101) in Figure 5.0. Figures 5.0a and b show that NRM and ARM behave similarly, suggesting that ARM is a good analog of NRM. This is true of all specimens. Figure 5.0c shows that SIRM also behaves similarly except that the recovery

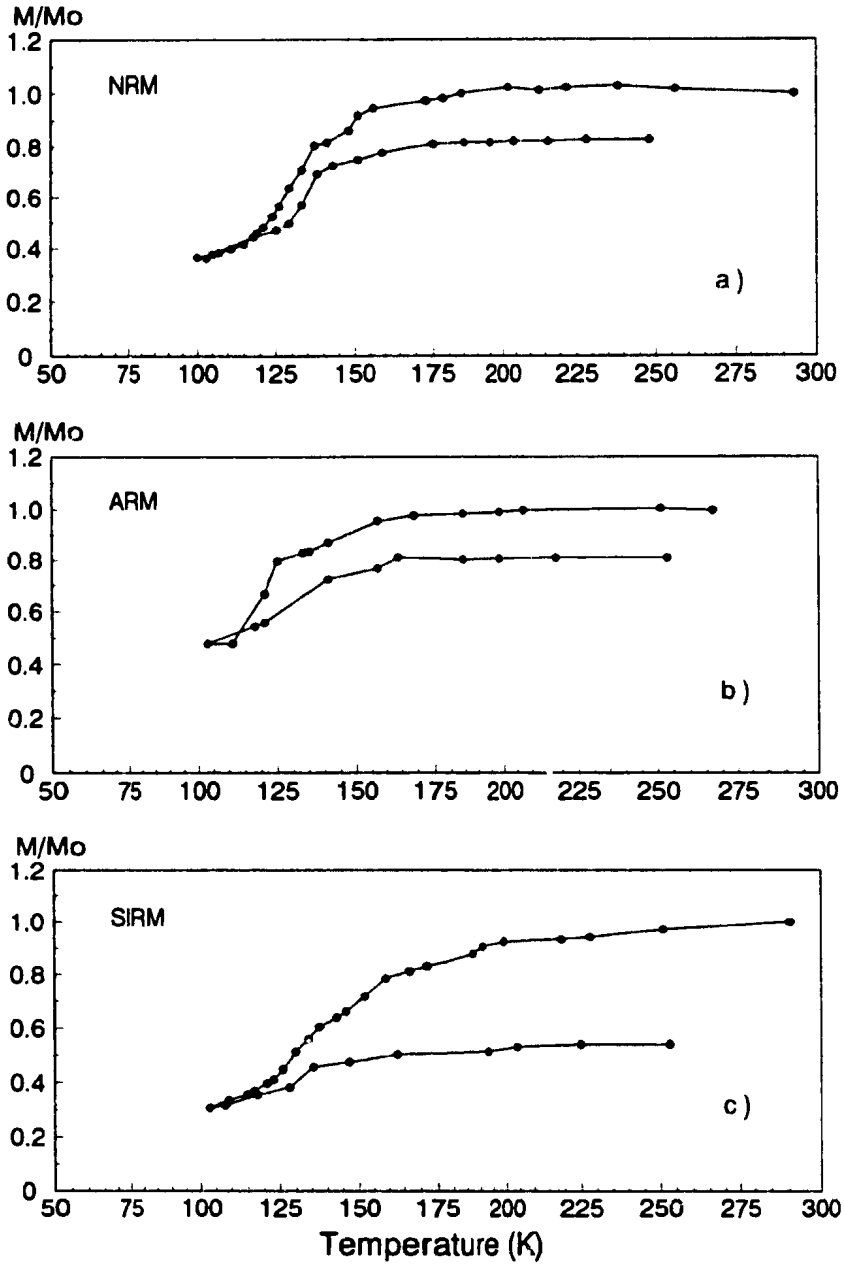

Fig 5.0 Specimen 3101

is less than for NRM or ARM. This is true of the rest of the specimens as well and is likely due to a higher portion of SIRM being controlled by weakly pinned domain walls, which is consistent with the MDFs of SIRM being lower than for NRM and ARM (Table 4.0). Clearly, ARM is superior to SIRM as an analog to NRM.

b.) Evidence for magnetostrictive control of remanence on cooling to the Verwey transition

Experimental evidence has been used by *Hodych* [1982a, 1986, 1990] and *Argyle and Dunlop* [1990] to argue that domain walls in MD magnetite can be pinned by magnetoelastic energy. *Heider et al.* [1992] experimentally and *Xu and Merrill* [1992] and *Moskowitz* [1993] theoretically showed that stress fields associated with dislocations in magnetite can cause magnetoelastic interaction with domain walls. Domain walls may also be K_1-controlled [*Merrill*, 1970]. *Hodych* [1991] showed that SIRM (and H_c) of many of his rock specimens decreased in rough proportion to λ_s on cooling, and concluded that remanence was likely magnetostrictively controlled in these rocks. We shall look for similar evidence of magnetoelastic control of remanence in our rocks.

Figures 5.1 and 5.2 represent the normalized thermal variation of ARM for all specimens discussed in *Section 5.3a* of this thesis. ARM rather than SIRM was chosen since it is a better analog for NRM. The smooth curve in each figure is the thermal variation of λ_{111} for pure magnetite measured by *Syono* [1964] and will be used instead of the Akulov relation for saturation polycrystalline magnetostriction λ_s, (where $\lambda_s = 0.4\lambda_{100} + 0.6\lambda_{111}$) since the thermal variation is largely due to λ_{111}, not to λ_{100} [*Xu and*

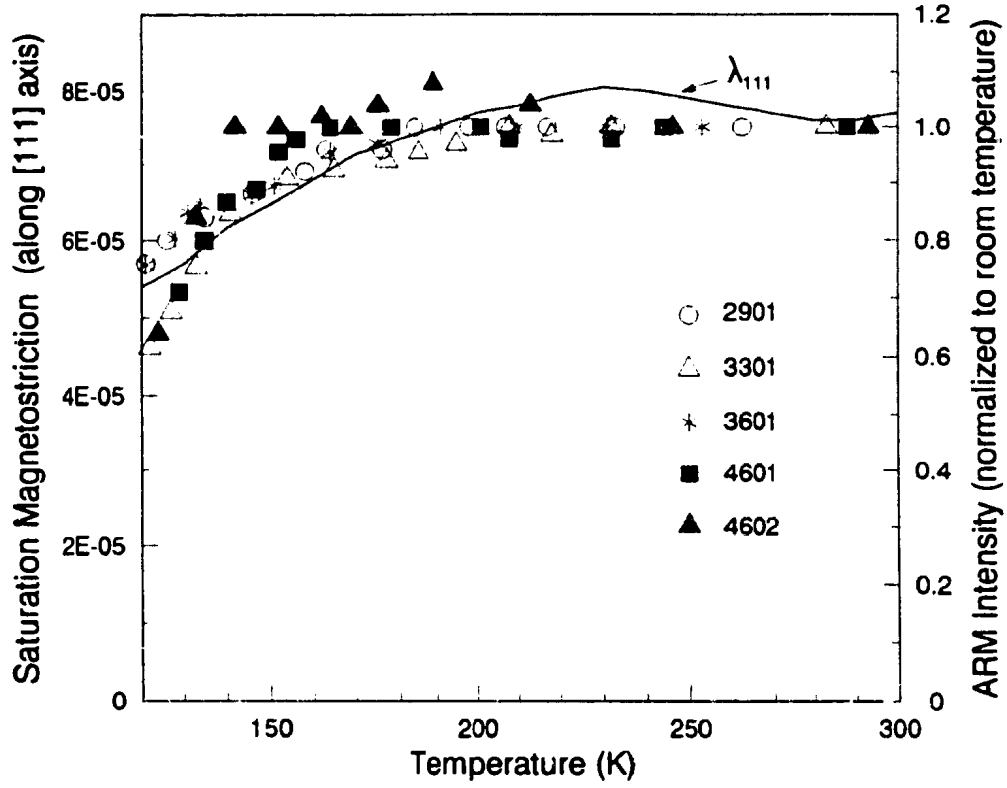

Fig 5.1 Change of ARM on cooling compared to magnetostriction for specimens with the Curie point of pure magnetite and remanence likely controlled magnetoelastically

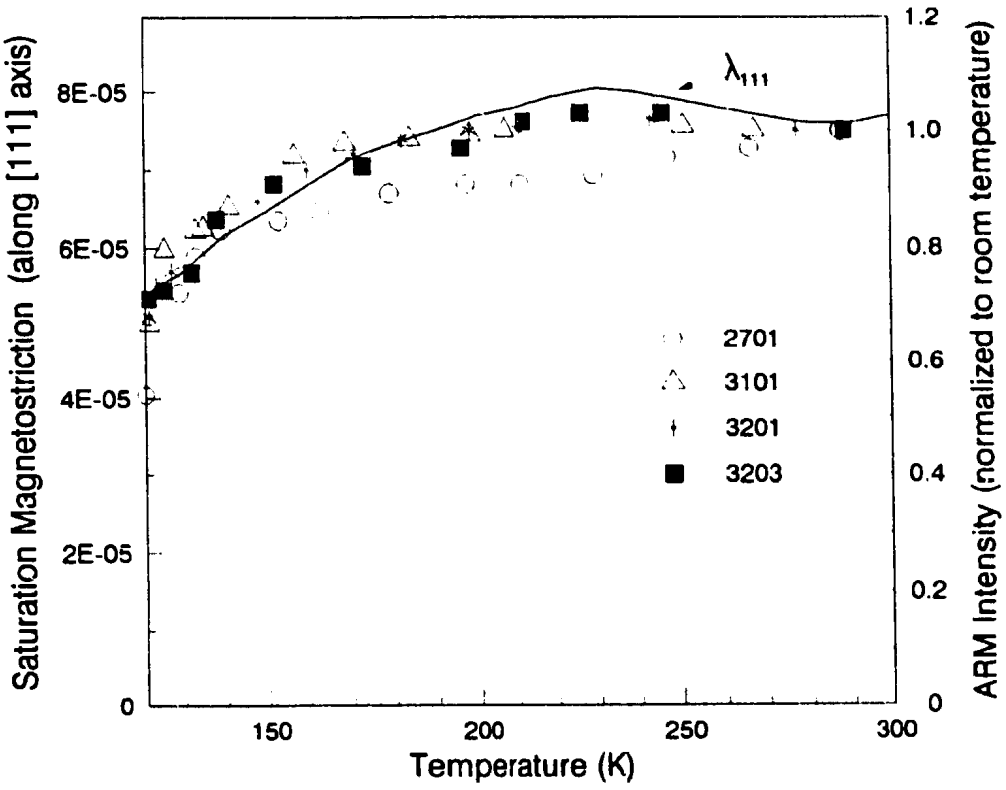

Fig 5.2 Change of ARM on cooling compared to magnetostriction for specimens with magnetite of small Ti content and remanence likely controlled magnetoelastically

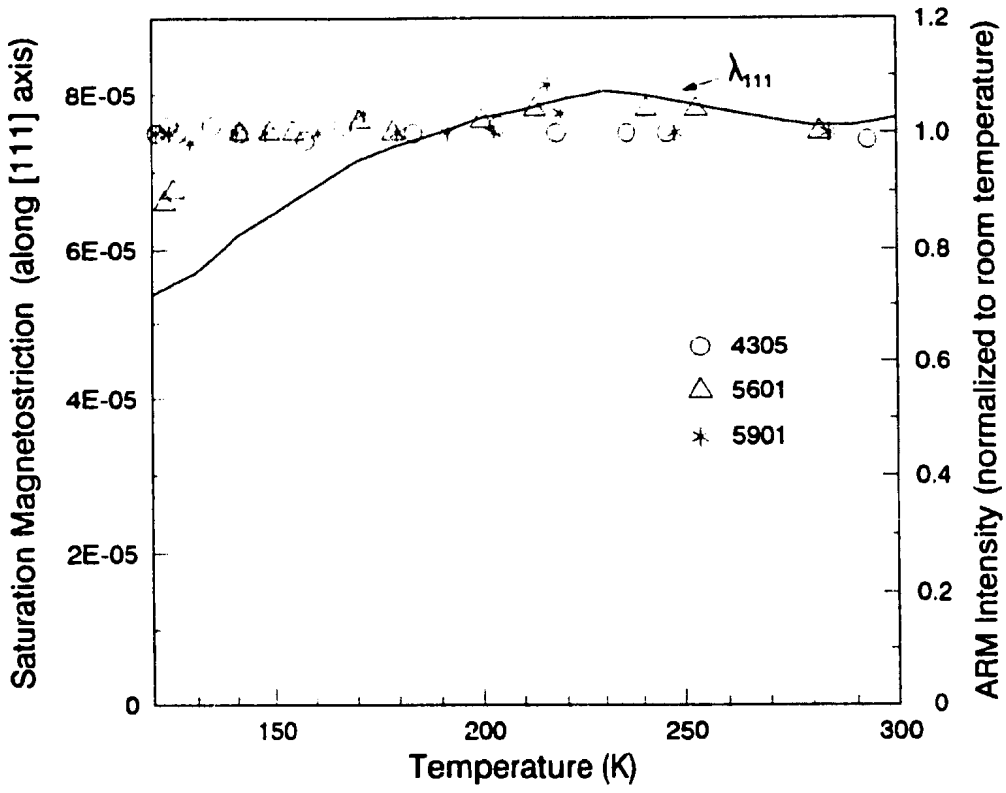

Fig 5.3 Change of ARM on cooling compared to magnetostriction for specimens with remanence likely controlled by shape anisotropy

Merrill, 1992].

Figure 5.1 and Figure 5.2 show specimen whose Curie points are 580°C and 560°C (or 540°C) respectively. The decrease of ARM on cooling roughly parallels decrease in λ_{111} suggesting magnetoelastic control of domain walls.

In contrast, Figure 5.3 shows the change of ARM on cooling for specimens 5901, 5601 and 4305. As already discussed in *Section 5.2*, there is comparatively little variation of ARM on cooling for these specimens suggesting remanence of these specimens is controlled by shape anisotropy.

c.) Effect of the Verwey transition

Hodych [1990] assumed that the drop in remanence intensity on cooling near the Verwey transition ($T_v \approx$ 110-120 K) was caused by a dramatic reorganization of domain walls, due to the dramatic change in magnetocrystalline anisotropy. The high magnetocrystalline anisotropy below T_v presumably prevents much remanence decrease on further cooling past T_v. However on warming back, this remanence is partially recovered after passing through T_v. The amount of recovery is expected to depend on the amount of internal stresses [*Kobayashi and Fuller*, 1968; *Heider et al.*, 1992]. Stressed regions of the grain, where domain walls are magnetoelastically pinned, are thought to cause remanence to recover after warming through T_v, whereas remanence due to K_1-controlled domain walls is permanently demagnetized on cooling through either T_k or T_v [*Heider et al.*, 1992].

Figure 5.4 shows the observed temperature of the greatest change in rate of SIRM

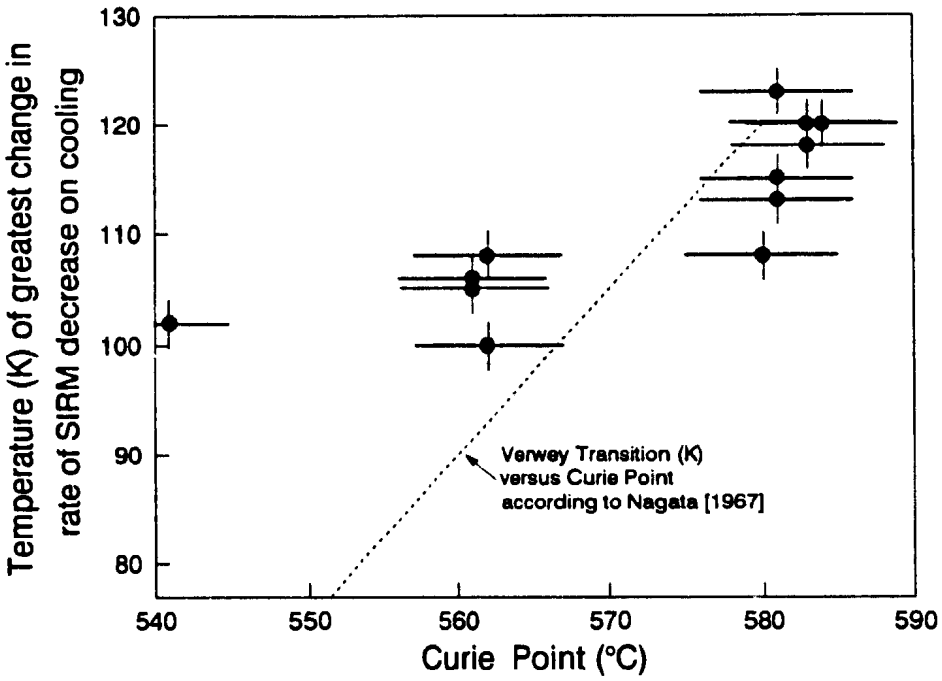

Fig 5.4 Temperature of the greatest change in rate of SIRM decrease on cooling plotted versus Curie Point

decrease on cooling (expected to equal T_v) plotted against Curie point. The dashed line represents approximately how T_v is observed to vary with Curie point from observations of *Nagata* [1967] of how T_v and T_c vary with Ti content. The temperature of greatest change in the rate of remanence decrease on cooling does seem to coincide with T_v (within errors of measurement) for most of the specimens, when variation of T_v with Ti content is thus taken into account.

5.4 Relationship between recovery after low-temperature cycling and median destructive fields

Figure 5.5 a and b is a plot of recovery of ARM and SIRM respectively versus median destructive fields for all the specimens studied in this thesis, along with reported data from *Heider et al.* [1992] and *Dunlop and Argyle* [1990] and *Levi and Merrill* [1976]. Recovery increases with median destructive field. This is consistent with magnetoelastic control of remanence since it is believed that recovery is due to internal stresses such as those caused by dislocations [*Heider et al.*, 1992], and recovery and median destructive field would both be expected to increase as dislocation density increases. Recovery would be expected to "saturate" at 100% for SD grains dominated by shape anisotropy.

Another possible explanation is that perhaps magnetite grain size is decreasing as median destructive field and recovery increases. *Heider et al.* [1992] showed that recovery increases with decreasing grain size and median destructive field should increases with decreasing grain size [*Dunlop*, 1990].

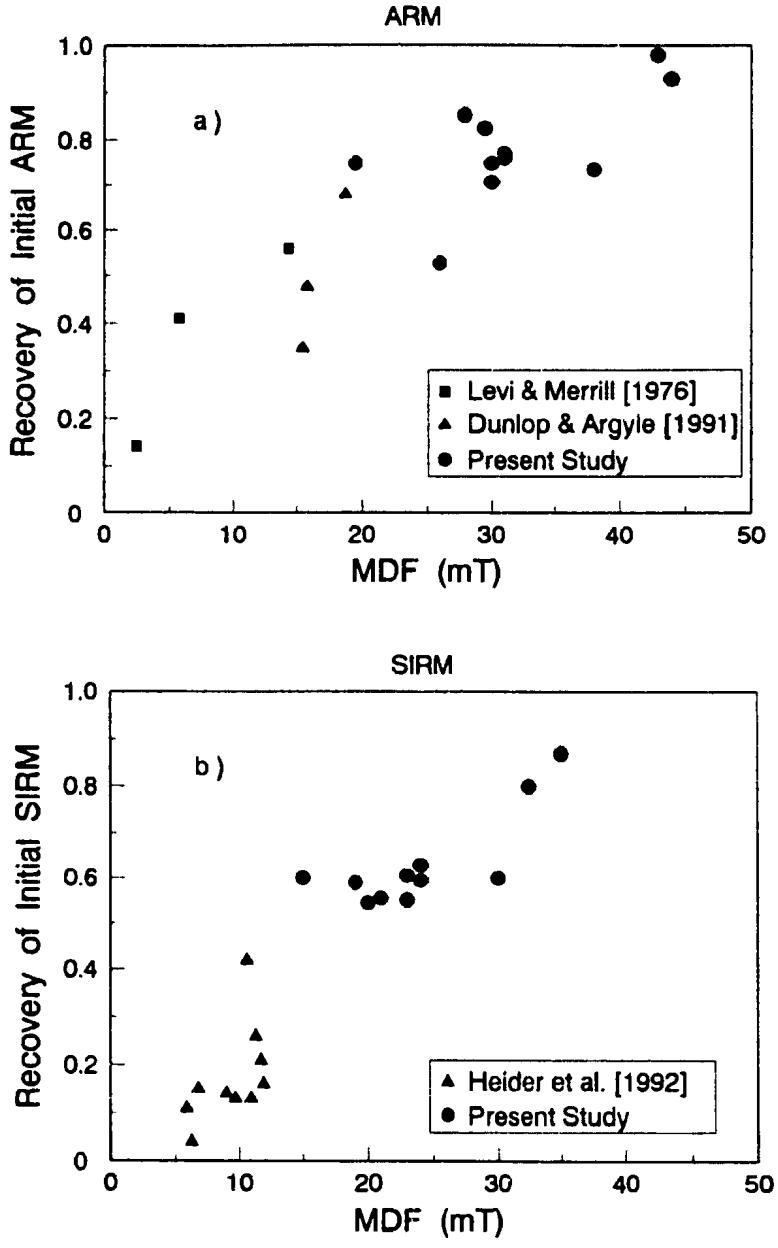

Fig 5.5 Recovery vs. Mean Destructive Field

5.5 Conclusions

(1) Dolerite block samples were collected at 39 sites in a dyke swarm near Nain, Labrador, with a U-Pb baddeleyite age of $1,277 \pm 3$ Ma. To determine the paleomagnetic viability of these dolerites, cylindrical specimens from each site had been step-wise AF-demagnetized. Of the initial 39 specimens, 21 carried a stable westerly direction of remanence which is likely primary. The 12 stable specimens that had AF-curves exhibiting quadratic decay (Figures 4.0d to 4.11d) were selected for low-temperature demagnetization.

(2) Observation of the decrease in remanence intensity on cooling in field-free space can help identify the possible mechanism controlling stability of remanence. Hence an apparatus was constructed to measure remanence while cooling from room temperature to 100 K and then warming back to room temperature, in field-free space. This apparatus was tested to ensure that specimen temperature and intensity of remanence could be reliably measured.

(3) For the 3 specimens (4305, 5601 and 5901) with the highest median destructive fields low-temperature cycling of NRM, ARM and then SIRM had little effect on remanence until the Verwey crystallographic transition ($T_v \approx 120$), where a small remanence decrease was evident. On warming back to room temperature, remanence recovered most of its initial remanence intensity. Lack of substantial net change in

remanence after a low-temperature cycle was also observed in .215μm and .390μm synthetic magnetite by *Dunlop and Argyle* [1991] and in < .31μm synthetic magnetite by *Levi and Merrill* [1976]. This behaviour coupled with high median destructive fields (~ 40mT) suggest that the remanence of specimens 4305, 5601 and 5901 is governed by shape anisotropy.

(4) The other 9 specimens showed pronounced decrease in NRM, ARM and SIRM on cooling to 100 K. Five of these specimens abruptly slowed their rate of decrease on passing through about 120 K, the Verwey transition temperature expected of pure magnetite (these five specimens had the 580°C Curie point expected of pure magnetite). The other four specimens continued their rapid decrease in remanence intensity on cooling past 120 K, presumably because T_v was shifted to lower temperatures because of the absence of titanium in the magnetite (these four specimens had Curie points lower than 580°C suggesting some titanium in their magnetite.) On warming back to room temperature, only a fraction of the initial remanence was recovered. Recovery of SIRM was usually less than recovery of NRM and ARM, which is consistent with a lower median destructive field for SIRM than for of NRM and ARM. Remanence stability in these specimens (whose median destructive fields varied between 18mT and 39.5mT) was likely due to controls on domain wall motion rather than to shape anisotropy.

(5) In the above 9 specimens, the decrease of ARM with temperature on cooling to near T_v roughly paralleled the decrease of λ_{111} (Figures 5.1 and 5.2). This suggests that domain wall motion may be magnetoelastically controlled, perhaps by dislocations.

(6) Recovery (remanence intensity after cooling cycle as a ratio of initial remanence) is shown to increase with median destructive field for our specimens and the specimens of *Levi and Merrill* [1976], *Dunlop and Argyle* [1991] and *Heider et al.* [1992], (*see Figures 5.5a and b*). This might be due to an increase in both recovery and median destructive field with increasing dislocation density.

References

Aragon, R., D.J. Buttrey, J.P. Shepherd and J.M. Honig. Influence of nonstoichiometry on the Verwey transition. *Phys. Rev.*, 31, 430-436, 1985.

Argyle, K.S. and D.J. Dunlop. Low-temperature and high-temperature hysteresis of small multidomain magnetites. *J. Geophys. Res.*, 95, 7069-7083, 1990.

Borradaile, G.J.. Low-temperature demagnetization and ice-pressure demagnetization in magnetite and haematite. *Geophys. J. Int.*, 116, 571-584, 1994.

Boyd, J. R., M. Fuller and S. Halgedahl. Domain wall nucleation as a controlling factor in the behaviour of fine particles in rocks. *Geophys. Res. Lett.*, 11, 193-196, 1984.

Buchan, K.L. and H.C. Halls. Paleomagnetism of Proterozoic mafic dyke swarms of the Canadian Shield (p209-230). In: A.J. Parker, P.C. Rickwood and D.H. Tucker (Editors). *Mafic Dykes and Emplacement Mechanisms.* Bulkema (Rotterdam), 541p., 1990.

Butler, R.F., Paleomagnetism. Blackwell. 319p., 1992.

Creer, K.M.. Rock magnetic investigations at low temperatures. In: D.W. Collinson, K.M. Creer and S.K. Runcorn (Editors). *Methods in Paleomagnetism*. Elsevier, Amsterdam, pp. 515-528, 1967.

Dankers, P. and N. Sugiura. The effects of annealing and concentration on the hysteresis properties of magnetite around the PSD-MD transition. *Earth Planet. Sci. Lett.*, 56, 422-428, 1981.

Day, R.. TRM and its variation with grain size. *J. Geomag. Geoelectr.*, 29, 233-265, 1977.

Dunlop, D.J.. Hysteresis properties of magnetite and their dependence on particle size : A test of pseudo-single-domain remanence models. *J. Geophys. Res.*, 91, 9569-9584, 1986.

Dunlop, D.J. and K.S. Argyle. Separating multidomain and single-domain-like re manences in pseudo-single-domain magnetites (.215-.540μm) by low-temperature demagnetization. *J. Geophys. Res.*, 96, 2007-2017, 1991.

Dunlop, D.J., J.A. Hanes and K.L. Buchan. Indices of multidomain magnetic behaviour in basic igneous rocks : Alternating-field demagnetization, hysteresis, and oxide petrology. *J. Geophys. Res.*, 78, 1378-1393, 1973.

Dunlop, D.J.. Developments in rock magnetism. *Rep. Prog. Phys.*, 53, 707-792, 1990.

Evans, M.E. and M.W. McElhinny. An investigation of the origin of stable remanence in magnetite bearing igneous rocks. *J. Geomagn. Geoelectr.*, 21, 757-772, 1969.

Fuller, M.D. and K. Kobayashi. Identification of magnetic phases carrying natural remanent magnetization in certain rocks. *J. Geophys. Res.*, 69, 4409-1413, 1964.

Heider, F.. Temperature dependence of the domain structure in natural magnetite and its significance for multidomain TRM models. *Phys. Earth Planet. Int.*, 65, 54-61, 1990.

Heider, F., S.L. Halgedahl and D.J. Dunlop. Temperature dependence of magnetic domains in magnetite crystals. *Geophys. Res. Lett.*, 15, 499-502, 1988.

Heider, F., D.J. Dunlop and H.C. Soffel. Low-temperature and alternating field demagnetization of saturation remanence and thermoremanence in magnetite grains (0.037μm to 5mm). *J. Geophys. Res.*, 97, 9371-9381, 1992.

Hodych, J.P.. Magnetostrictive control of coercive force in multidomain magnetite. *Nature*, 298, 542-544, 1982.

Hodych, J.P.. Evidence for magnetostrictive control of intrinsic susceptibility and coercive force of multidomain magnetite in rocks. *Phys. Earth Planet. Int.*, 42, 184-194, 1986.

Hodych, J.P.. Magnetic hysteresis as a function of low temperature in rocks: evidence for internal stress control of remanence in multi-domain and pseudo-single-domain magnetite. *Phys. Earth Planet. Int.*, 64, 21-36, 1990.

Hodych, J.P.. Low-temperature demagnetization of saturation remanence in rocks bearing multidomain magnetite. *Phys. Earth Planet. Int.*, 66, 144-152, 1991.

Jarrard, R.D. and S.L. Halgedahl. Large discontinuous magnetization jumps associated with the low-temperature transition of magnetite (abstract). *Eos Trans. AGU*, 71, 486, 1990.

Kakol, K., J. Sabol and J.M. Honig. Magnetic anisotropy of titanomagnetites $Fe_{3-x}Ti_xO_4$, $0 \leq x < 1$. *Phys. Rev.*, 44, 2198-2204, 1991.

Kittel, C.. Physical theory of ferromagnetic domains. *Rev. Mod. Phys.*, 21, 541-583, 1949.

Kobayashi, K. and M. Fuller. Stable remanence and memory of multidomain materials with special reference to magnetite. *Philos. Mag.*, 18, 601-624, 1968.

Landau, L. and L. Lifshitz. On the theory of dispersion of magnetic permeability in ferromagnetic bodies. *Phyz. Z.*, 8, 153-169, 1935.

Levi, S. and R.T. Merrill. A comparison of ARM and TRM in magnetite. *Earth Planet. Sci. Lett.*, 32, 171-184, 1976.

Levi, S. and R.T. Merrill. Properties of single-domain, pseudo-single-domain, and multidomain magnetite. *J. Geophys. Res.*, 83, 309-323, 1978.

Lowrie, W. and M. Fuller. Effect of annealing on coercive force and remanent magnetizations in magnetite. *J. Geophys. Res.*, 74, 2698-2710, 1969.

Lowrie, W. and M. Fuller. On the alternating field demagnetization characteristics of multidomain thermoremanent magnetization in magnetite. *J. Geophys. Res.*, 76, 6339-6349, 1971.

Mauritsch, H.J. and P. Turner. The identification of magnetite in limestones using the low-temperature transition. *Earth. Planet. Sci. Lett.*, 24, 414-418, 1975.

Merrill, R.T.. Low temperature treatments of magnetite and magnetite-bearing rocks. *J. Geophys. Res.*, 75, 3343-3349, 1970.

Moon, T. and R.T. Merrill. Single domain theory of remanent magnetization. *J. Geophys. Res.*, 93, 9202-9210, 1988.

Moskowitz, B.M.. Micromagnetic study of the influence of crystal defects on coercivity in magnetite. *J. Geophys. Res.*, 98, 18,011-18,026, 1993.

Moskowitz, B.M., R. Frankel, D.A. Bazylinski, H.W. Jannasch and D.R. Lovley. A comparison of magnetite particles produced anaerobically by magnetotatic and dissimilarly iron-reducing bacteria. *J. Geophys. Res. Lett.*, 16, 665-668, 1989.

Nagata, T., K. Kobayashi and M.D. Fuller. Identification of magnetite and hematite in rocks by magnetic observation at low temperature. *J. Geophys. Res.*, 69, 2111-2120, 1964.

Nagata, T.. Identification of magnetic minerals in rocks using methods based on their magnetic properties. In: D.W. Collinson, K.M. Creer and S.K. Runcorn (Editors). *Methods in Paleomagnetism*. Elsevier, Amsterdam. pp. 501-513, 1967.

Neel, L.. Theorie du Trainge magnetique des ferromagnetiques en grains fins avec applications aux terres cuties. *Ann. Geophys.*, 5, 99-136, 1949.

Özdemir, O., D.J. Dunlop and B.M. Moskowitz. The effect of oxidation on the Verwey transition in magnetite. *Geophys. Res. Lett.*, 20, 1671-1674, 1993.

Ozima, M., M. Ozima and T. Nagata. Low-temperature treatment as an effective means of "magnetic cleaning" of natural remanent magnetization. *J. Geomag. Geoelectr.*, 16, 37-40, 1964.

Pauthenet, R.. Variation thermique de l'aimantation spontanee des ferrites de nickel, cobalt, fer et manganese. *Compt. R. Acad. Sci. Paris*, 230, 1842-1843, 1950.

Parry, L.G.. Magnetization of multidomain particles of magnetite. *Phys. Earth Planet. Int.*, 19, 21-30, 1979.

Parry, L.G.. Shape-related factors in the magnetization of immobilized magnetite particles. *Phys. Earth Planet. Int.*, 22, 144-154, 1980.

Schmidbauer, E. and Schembera. Magnetic hysteresis properties and anhysteretic remanent magnetization of spherical Fe_3O_4 particles. *Phys. Earth Planet. Int.*, 46, 64-70, 1987.

Shive, P.N.. The effect of internal stress on the thermoremanence of nickel. *J. Geophys. Res.*, 74, 3781-3788, 1969.

Shive, P.N. and R.F. Butler. Stress and magnetostrictive effects of lamellae in titanomagnetite and ilmenohematite series. *J. Geomagn. Geoelectr.*, 21, 781-796, 1969.

Smith, G.M. and R.T. Merrill. Annealing and stability of multidomain magnetite. *J. Geophys. Res.*, 89, 7877-7882, 1984.

Strangway, D.W., E.E. Larson and M. Goldstein. A possible cause of high magnetic stability in volcanic rocks. *J. Geophys. Res.*, 73, 3787-3795, 1968.

Stacey, F.D.. The physical theory of rock magnetism. *Adv. Phys.*, 12, 45-133, 1963.

Syono, Y.. Magnetocrystalline anisotropy and magnetostriction of Fe_3O_4-Fe_2TiO_4 series - with special application to rock magnetism. *Jpn. J. Geophys.*, 4, 71-143, 1965.

Tarling, D.H.. *Palaeomagnetism*. Chapman and Hall, 378 pp., 1983.

Verhoogen , J.. The origin of thermoremanent magnetization. *J. Geophys. Res.*, 64, 2441-2449, 1959.

Verwey, E.J.W.. Electronic conduction of magnetite (Fe_3O_4) and its transition point at low temperatures. *Nature*, 144, 327-328, 1939.

Worm, H.U. and H. Markert. The preparation of dispersed titanomagnetite particles by the glass-ceramic method. *Phys. Earth Planet. Int.*, 46, 263-269, 1987.

Xu, S. and R.T. Merrill. Microstress and microcoercivity in multidomain grains. *J. Geophys. Res.*, 94, 10627-10636, 1989.

Xu, S. and R.T. Merrill. Microcoercivity, bulk coercivity and saturation remanence in multidomain materials. *J. Geophys. Res.*, 95, 7083-7090, 1990a.

Xu, S. and R.T. Merrill. Stress, grain size and magnetic stability of magnetite. *J. Geophys. Res.*, 97, 4321-4329, 1992.

Zuo, J.M. et al.. Charge ordering in magnetite at low temperatures. *Phys. Rev.*, 42, 8451-5464, 1990.